Studies on Peripheral Blood mMDSC Based-Biomarker Exploration and a Novel Therapeutic Agent for Cancer Immunotherapy

August 2021

Kenna SHIRASUNA

Studies on Peripheral Blood mMDSC Based-Biomarker Exploration and a Novel Therapeutic Agent for Cancer Immunotherapy

A Dissertation Submitted to

the School of the Integrative and Global Majors,

the University of Tsukuba

in Partial Fulfillment of the Requirements

for the Degree of Doctor of Philosophy in Disease Mechanism

(Doctoral Program in Life Science Innovation)

Kenna SHIRASUNA

Abstract

Cancer is the second leading of cause of death worldwide. In 2020, it is estimated that 19.3 million people were newly diagnosed with cancer and almost 10 million people died from their pre-existing disease. In the past, treatment strategies for cancer patients have been based primarily on surgery, chemotherapy and radiation therapy. Now, however, immunotherapy using antibodies specific for immune checkpoint molecules (e.g., anti-programmed death-1 (anti-PD-1) and anti-cytotoxic T lymphocyte antigen 4 (anti-CTLA-4)), has emerged as a novel and powerful treatment. Immune checkpoint inhibitor (CPI) therapy shows superior overall survival in advanced malignancies including melanoma and lung cancers, compared to conventional therapies. Unfortunately, most patients (about 80%) still do not benefit from CPI therapy as a monotherapy, and the potential for serious side effects exists. Therefore, to optimize selection of suitable patients for CPI therapy and avoid iatrogenic toxicity, there is a need for new biomarkers.

Monocytic myeloid-derived suppressor cells (mMDSCs) are a class of immunosuppressive immune cells with prognostic value in many solid tumor cases. The proportion of mMDSCs in the peripheral blood appears to be a prognostic marker that

can indicate a positive response to CPI therapy. However, measuring peripheral mMDSC levels is currently difficult in current medical practice because of the need for specialized equipment (e.g., flow cytometry) and the instability of mMDSCs. Therefore, establishing a simple method to determine the levels of peripheral mMDSC would be of significant clinical benefit. As a step towards doing so in colorectal cancer (CRC) patients, I performed a correlation analysis of the proportion of mMDSCs in freshly-drawn peripheral blood with levels of plasma proteins (cytokines, chemokines, growth factors and enzyme) and demographic factors. Freshly drawn mMDSCs were measured using flow cytometry on PBMCs from healthy donors (n = 24) and CRC patients (n = 78). The plasma concentrations of 29 different cytokines, chemokines, growth factors, and enzymes were measured using a multiplex assay or enzyme-linked immunosorbent assay (ELISA). Correlation analysis to find mMDSC-associated factors was conducted using univariate and multivariate models. In univariate correlation analysis, there were no plasma proteins that were associated with mMDSC proportions in CRC patients. In multivariate analysis, considering all variables including age, gender, stage and plasma proteins, levels of inducible nitric acid synthase (iNOS) ($p = 0.013$) and platelet-derived

growth factor (PDGF)-BB ($p = 0.035$) were associated with mMDSC proportion in PBMCs (mMDSC proportion [%] = 0.2929 − 0.2389 * PDGF-BB + 0.3582 * iNOS) ($p < 0.005$, $r = 0.32$). Measuring the plasma concentrations of iNOS and PDGF-BB may be useful in predicting the proportion of mMDSCs in CRC patients' peripheral blood.

Biomarkers serve critical diagnostic and prognostic purposes, but they are not therapeutics. It is vital to develop a novel drugs effective in CPI-resistant patients, either as a monotherapy or in combination with CPIs. For example, in preclinical studies, targeting myeloid-derived suppressor cells (MDSCs) and regulatory T cells (Tregs) improves responses to anti-CTLA-4 and anti-PD-1 antibodies. T-cell immunoreceptor with immunoglobulin (Ig) and immunoreceptor tyrosine-based inhibitory motif domains (TIGIT) is a validated immune checkpoint molecule expressed on memory $CD4^+$T cells, Tregs, $CD8^+$T cells and natural killer (NK) cells. TIGIT binds to its ligands, poliovirus receptor (PVR) and poliovirus receptor-related 2 (PVRL2) expressed on cancer cells, MDSCs, and dendritic cells, producing an immunosuppressive signal for both the receptor- and ligand-expressing cells. Several groups have demonstrated that anti-TIGIT blocking antibody treatment abolished the immunosuppressive activity of MDSCs and

Tregs against $CD8^+$T cells. TIGIT signal blocking may be efficacious as a single agent in CPI resistant patients or have additive or synergistic effects with CPIs. I generated anti-TIGIT blocking antibodies (ASP8374: therapeutic antibody and mSEC1: mouse surrogate antibody) and investigated non-clinical studies. ASP8374 is a fully human monoclonal IgG4 antibody designed to block the interaction of TIGIT with its ligands and inhibit TIGIT signaling. ASP8374 bound with high affinity to TIGIT and increased interferon (IFN)-γ production by cultured PBMCs in a dose-dependent manner. When used in combination with pembrolizumab, an anti-PD-1 antibody, ASP8374 induced higher T cell activation *in vitro* than either treatment alone. A surrogate anti-mouse TIGIT antibody, mSEC1, was efficacious in an MC38 syngeneic colon tumor mouse model (anti-PD-1/ anti-programmed death-ligand 1 (PD-L1) antibody sensitive model [MDSC low model]) alone and in combination with anti-PD-L1 antibody. In an additional syngeneic colon tumor mouse model, CT26 (anti-PD-1/anti-PD-L1 antibody insensitive model [MDSC expansion model]), mSEC1 alone had no anti-tumor effect, but mSEC1 combined with an anti-PD-1 antibody augmented anti-tumor action of the anti-PD-1 antibody alone. These data provide evidence that ASP8374 has therapeutic potential to

amplify the activity of anti-PD-(L)1 antibodies in the clinic where PD-1 blockade is not fully efficacious.

Contents

Abbreviations

APCs	antigen presenting cells
CMV	cytomegalovirus
CPIs	immune checkpoint inhibitors
CRC	colorectal cancer
CTLA-4	cytotoxic T lymphocyte antigen 4
EC_{50}	half maximal effective concentration
ELISA	enzyme-linked immunosorbent assay
gMDSCs	granulocytic myeloid-derived suppressor cells
IC_{50}	half maximal inhibitory concentration
Ig	immunoglobulin
IHC	immunohistochemistry
iNOS	inducible nitric oxide synthase
ip	intraperitoneal
K_D	dissociation constant
MDSCs	myeloid-derived suppressor cells

mMDSCs monocytic myeloid-derived suppressor cells

NK cells natural killer cells

NO nitric oxide

PBMCs peripheral blood mononuclear cells

PD-1 programmed death 1

PDGF-BB platelet-derived growth factor BB

PD-L1 programmed death ligand 1

PD-L2 programmed death ligand 2

PVR poliovirus receptor

PVRL2 poliovirus receptor-related 2

TIGIT T-cell immunoreceptor with Ig and immunoreceptor tyrosine-based inhibitory motif domains

TILs tumor-infiltrating lymphocytes

TME tumor microenvironment

Tregs regulatory T cells

Chapter 1:

General Introduction

Cancer is the second leading of cause of death worldwide. In 2020, it is estimated that 19.3 million people were newly diagnosed with cancer and almost 10 million people died from their pre-existing disease [1]. Until recently, surgical resection, chemotherapy, and radiation therapy have been the three pillars of cancer treatment. In recent years, interest in immunotherapy has increased due, in part, to data showing that it can improve overall survival in some patients with treatment-resistant cancers. It thus has become the fourth pillar in cancer treatment. Wilhelm Busch and Friedrich Fehleisen were the first to posit an etiologic relationship between cancer and immunity [2]. They noticed that tumors spontaneously regressed in patients who had erysipelas, a common bacterial infection of the skin. Thereafter, William Coley, the "Father of Cancer Immunotherapy," showed that erysipelas correlated with a favorable prognosis in sarcoma patients through retrospective analysis [3]. To confirm the epidemiological evidence, he attempted to treat cancer patients with heat-inactivated *S. pyogenes* and *Serratia marcescens*, called "Coley's toxins" that could potentially activate an immune response [4]. Although Coley's toxins

caused complete remission in a variety of cancers, including sarcomas and testicular carcinomas, they never became a standard therapy due to lack of scientific evidence, reproducibility, and the risks of infecting patients intentionally with pathogenic bacteria. Surgery and radiation therapy were the standards of care in the early 20th century [2].

Soon after, the emergence of new technologies reinvigorated the cancer immunotherapy field. Several groups suggested that, although the tumor cells may arise spontaneously throughout life, they bore tumor-associated neoantigens that could be recognized by the immune system, which then would eliminate these cells. This “cancer immunosurveillance” hypothesis [2,3] was supported by studies in mouse tumor models that showed immune activation by adoptive transfer [4] and clinical data showing spontaneous tumor regression in melanoma patients who had autoimmune disease [5]. Gene knockout mouse models provided experimental proof of a link between carcinogenesis and immunodeficiency [6]. Furthermore, cancer-specific immune responses were identified by molecular and biochemical research approaches [7]. This evidence that the immune system could fight cancer stimulated research into cancer immunotherapy.

The next breakthrough in cancer immunotherapy was the discovery of negative regulators of immune cell activation, “inhibitory immune checkpoint molecules,” cell surface receptors that mediate the balance between immunosurveillance against abnormal cells or foreign antigens and autoimmunity [8]. CTLA-4 and PD-1, which are expressed on activated T cells, are the most promising examples of immune checkpoint molecules. Research on molecular mechanism of CTLA-4 and PD-1 was done by James P. Allison and Tasuku Honjo, respectively, who received the Nobel-Prize winners for Physiology or Medicine in 2018 [9]. CTLA-4 is a member of the immunoglobulin super family and exhibits inhibitory effects on T cell activation mainly via competition with CD28, costimulation molecule by binding to their shared ligands, CD80/CD86 expressed on the antigen-presenting cells (APCs), besides direct inhibitory function through the cytoplasmic domain that reacts with signaling molecules [10] (Fig. 1-1). Allison’s group showed that CTLA-4 knock-out mice induce T cell lymphoproliferation and develop a lethal autoimmune disorder, confirming the role of CTLA-4 as an inhibitory regulator of T cells. His group also studied the effect of CTLA-4 on tumor growth in immunocompetent mice and showed that anti-CTLA-4 blocking antibody inhibited tumor

growth [10]. PD-1 is a member of the B7/CD28 family and regulates T-cell immune response via interaction with PD-L1 and programmed death ligand 2 (PD-L2), which are expressed on APCs and tumor cells [10] (Fig. 1-1). As with CTLA-4 signaling, PD-1/PD-L1 (or PD-L2) signaling inhibits T cell activation [10]. Honjo's group reported that although PD-1 deficient mice are healthy at birth, after one year, they develop symptoms of autoimmune disease gradually begin to appear in the aged mice [10]. In addition to the functional analysis of PD-1 deficient mice, his group also indicated that PD-1 signal blockade inhibits tumor growth in immunocompetent mouse tumor models. These data point to the potential of the CPIs in cancer immunotherapy. The immune system is normally suppressed by inhibitory immune checkpoint molecules such as CTLA-4 and PD-1. The inhibitory effects of these molecules are vital to self-tolerance. Although tumor -recognizing cytotoxic T cells are generated and try to attack tumor cells, tumors may escape T cell immune surveillance by modulating these immune checkpoint pathways. CPI therapy seeks to remove signals inhibiting T cell activation by blocking the immune checkpoint molecules from binding with their ligands, which leads cytotoxic T cells to attack cancer cells (Fig. 1-1). Based on these findings, therapeutic anti-CTLA-4 and anti-

PD-1 blocking antibodies were developed by several pioneering groups [9]. In clinical trials, these antibodies were efficacious, dramatically improving survival by inducing immune activation against a variety of cancers that were unresponsive to conventional therapies. In 2011, ipilimumab was the first anti-CTLA-4 antibody (human IgG1) approved in the US (FDA) and EU (EMA) for advanced melanoma. In 2015, it was approved in Japan (PMDA) [9]. It is currently approved for several tumor indications worldwide. One of the most impressive indications of the efficacy of ipilimumab is the fact that 20% of advanced melanoma patients enrolled in the first ipilimumab clinical study are still alive [9]. For anti-PD-1 antibody, there are currently three approved drugs, Nivolumab (human IgG4), pembrolizumab (humanized IgG4) and cemiplimab (human IgG4). Nivolumab received drug approval for advanced melanoma from PMDA and FDA in 2014, and from EMA in 2015. Pembrolizumab was approved by FDA in 2014, EMA in 2015, and PMDA in 2016 for advanced melanoma. Cemiplimab was approved by FDA in 2018, EMA in 2019 for metastatic cutaneous squamous cell carcinoma (no approval in Japan at this moment). In clinical trials, nivolumab and pembrolizumab yield broader clinical responses than ipilimumab, and thus these two anti-PD-1 antibodies have

been used to treat other cancers, including colorectal cancer, lung cancer, renal cell carcinoma, Hodgkin lymphoma, head and neck squamous cell cancers, and melanoma [9].

Although anti-CTLA-4 and anti-PD-1 antibodies are the most promising immunotherapeutic approaches, unfortunately, about 80% of patients do not benefit from anti-CTLA-4 and anti-PD-1 antibody therapy (current CPI therapy) and, in addition, serious side effects have been reported [11]. The most common side effects are diarrhea, fatigue, itching, and pneumonitis, all of which are immune-related side effects. Although the frequency of immune-related side effects depends on the type of CPI and the type of cancer, approximately 50% of patients treated with anti-CTLA4 antibody and 30% of patients treated with anti-PD-1 antibody develop side effects [12]. Therefore, to properly stratify patients and reduce medical costs, there is a growing need for specific biomarkers. In current CPI therapy, tumor-infiltrating lymphocytes (TILs), tumor PD-L1 expression, tumor mutational burden, inflammatory gene expression, and other factors all are being considered. For anti-PD-(L)1 antibody treatment, the only FDA approved test is based on the immunohistochemistry (IHC) for PD-L1 detection at the tumor site [13]. More

biomarkers are needed because many other factors may correlate with tumor response. Markers in peripheral blood would be especially useful because of the ease with which blood can be drawn and the relatively simple instrumentation required.

A useful prognostic biomarker used in ipilimumab and nivolumab therapy is the proportion of peripheral mMDSCs [14,15]. mMDSCs are a heterogenous population of immature myeloid cells that suppress responses of immune cells such as T cells, NK cells and dendritic cells [16,17] (Fig. 1-2). The number of circulating mMDSCs is increased in patients with various type of cancers such as melanoma, breast cancer, and CRC, and is inversely correlated with clinical outcome [18,19]. In metastatic melanoma patients who were treated with ipilimumab, responders had a lower proportion of peripheral mMDSCs compared to non-responders [14]. Low numbers of mMDSCs also inversely correlates with outcomes in melanoma patients treated with nivolumab [15].

Although the proportion of peripheral blood mMDSCs is a useful biomarker, determining this proportion requires freshly drawn blood (freezing affects results) and flow cytometry with multicolor staining [20]. In addition, mMDSCs are defined as $CD14^{+}HLA\text{-}DR^{-/low}$ cells in humans and their HLA-DR expression often varies, and in

addition, identification of a specific subset of cells is susceptible to inter-user, intra-day, and inter-laboratory variability. Standardization thus is an issue. For these reasons, there is a need for a simpler, more accurate method of determining peripheral mMDSC proportions. In Chapter 2, I report results from a correlation analysis of the proportion of freshly-drawn peripheral mMDSCs, levels of different plasma proteins, and demographic factors (age and gender) in CRC patients.

In the treatment of cancers, biomarkers are clinically useful, but they themselves are not therapeutic in the usual sense of the word. Therefore, it is vital to develop new drugs that can help CPI-resistant patients, either as monotherapy or to augment CPIs. Although the mechanism of CPI therapy resistance remains to be fully elucidated, it is known that increased numbers of immune suppressive cells, such as MDSCs and Tregs, are involved (Fig. 1-2). Targeting MDSCs and Tregs improved responses to CPIs in animal models [21–25]. Thus, MDSCs and Tregs are potential targets for current CPI resistant patients. Other novel inhibitory checkpoint molecules have been discovered. For example, one of the new generation of check point molecules is TIGIT, which has been implicated in tumor immunosurveillance [26]. TIGIT is mainly expressed on T cells, NK cells and

Tregs. TIGIT binds to its ligands, PVR and PVRL2 which are expressed on cancer cells, MDSCs and dendritic cells, leading to induction of an immunosuppressive signal in both the receptor- and ligand-expressing cells (Fig. 1-3). Immunosuppressive activity of MDSCs and Tregs against $CD8^+$T cells can be abolished by anti-TIGIT blocking antibody [27–29] and diminished tumor cell killing activity of NK cells cocultured with MDSCs can be reversed by TIGIT signal blocking [30]. Both TIGIT and PD-1 are co-expressed on T cells in the tumor microenvironment (TME) in a wide variety of cancer patients [31]. TIGIT signal blocking thus may be effective as a monotherapy for anti-PD-(L)1 antibody resistant patients, or to augment the effects of anti-PD-(L)1 antibodies. In Chapter 3, I discuss my production of anti-TIGIT blocking antibodies (ASP8374: therapeutic antibody and mSEC1: mouse surrogate antibody) and the results of pharmacological studies of their activity for monotherapy and for combination therapy with anti-PD-(L)1 antibodies.

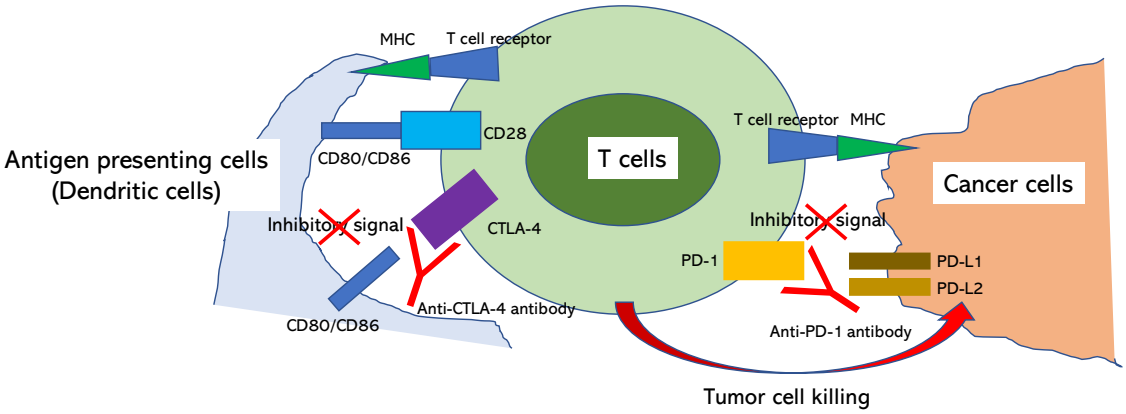

Fig. 1-1 Mechanism of actions of anti-CTLA-4 and anti-PD-1 antibodies

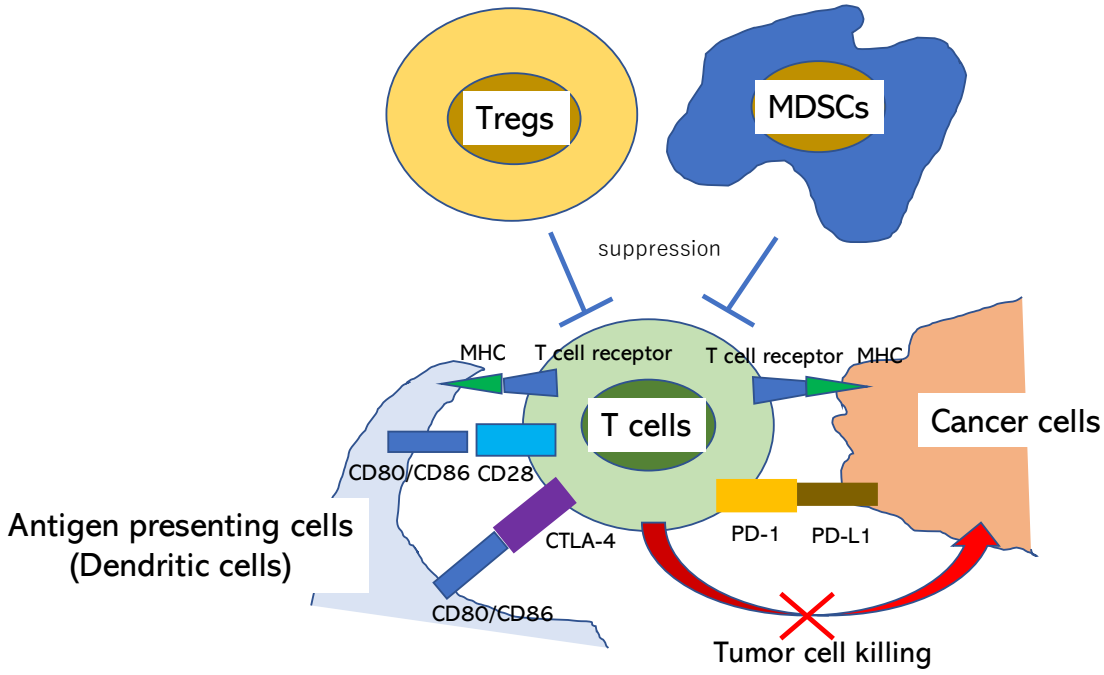

Fig. 1-2 Immunosuppression mediated by MDSCs and Tregs

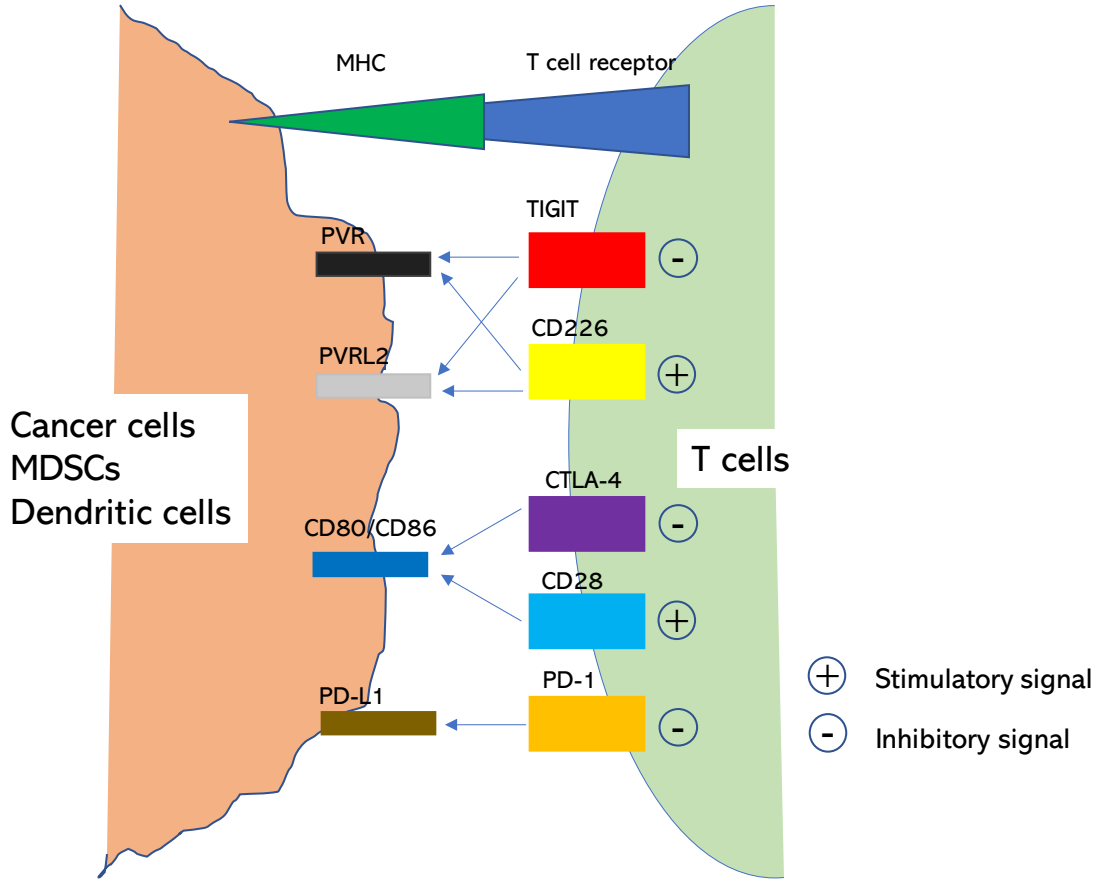

Fig. 1-3 Mechanism of action of TIGIT

Chapter 2:

Correlation Analysis of the Proportion of mMDSCs in CRC Patients

Introduction

There were approximately 1.1 million new CRC cases and 551,269 CRC deaths worldwide in 2018 [32]. Previous studies have demonstrated that chronic inflammation is necessary for the initiation of CRC pathogenesis. CRC-related inflammation promotes tumor development and progression through many different mechanisms, such as promoting angiogenesis and suppressing anti-tumor immune responses. A chronic inflammatory mucosal microenvironment can also trigger oncogenic mutations that serve as CRC-initiating events [33]. Further tumor progression is induced by inflammatory immune cells, which also work to turn an inflamed microenvironment into an immunosuppressive one [34]. It has been reported that CRC induces inflammatory immune cell infiltrates through upregulation of “inflammatory signature” genes [33,34]. Infiltration of $CD4^+$T cells and $CD8^+$ T cells is associated with a good prognosis in CRC

[35–37]. However, Tregs and immunosuppressive myeloid cells are associated with a poor prognosis [33,34], thus characterizing these immunosuppressive cells accurately is crucial for diagnosis and therapy of CRC.

MDSCs, a subset of immune suppressive cells, are a heterogeneous population of immature myeloid lineage cells [16,17]. Human MDSCs are classified into two groups, $CD15^+$ granulocytic MDSCs (gMDSCs) and $CD14^+$ mMDSCs. Both groups of MDSCs have been shown to suppress immune responses through multiple mechanisms. These include production of nitric oxide (NO) through iNOS, release of reactive oxygen species (ROS), depletion of arginine by arginase, secretion of immunosuppressive cytokines such as transforming growth factor-β (TGF-β) and interleukin-10 (IL-10), and inducing apoptosis mediated by the Fas antigen-Fas ligand (FAS-FASL) pathway [38–43]. gMDSCs express high levels of arginase and ROS, whereas mMDSCs express high levels of both arginase and iNOS but express less ROS [44,45]. Peripheral mMDSCs inhibit the NY-ESO-1 melanoma antigen-specific T cell response to tumor cells *in vitro*, are associated with clinical cancer stage, and show prognostic value for overall survival in melanoma patients [46]. Several groups have also demonstrated that the proportion of

peripheral mMDSCs is significantly increased in patients with breast cancer and CRC, and correlates positively with clinical cancer stage, tumor burden, and poor clinical outcomes [18,19].

Although measuring the proportion of peripheral mMDSCs is beneficial to predict clinical outcome in cancer patients, it requires a complex process of flow cytometric analysis with detection of multiple cell surface markers. In addition, though mMDSCs are characterized as $CD14^{+}HLA\text{-}DR^{-/low}$ cells in humans, their HLA-DR expression typically shows variability, making identification of a specific subset of cells susceptible to inter-user and intra-day variability. For these reasons, measuring peripheral mMDSC levels using this method would be difficult to develop as a basic clinical test. In an effort to identify new biomarkers, I performed a comprehensive correlation analysis of the proportion of peripheral mMDSCs with plasma levels of multiple proteins and with demographic factors such as age, gender, and clinical grade of CRC. I found that the levels of peripheral mMDSC correlate with those of iNOS and PDGF-BB. Further research is required to validate and standardize these biomarkers, but they have potential as prognostic indicators that would be of benefit during immunotherapy.

Materials & Methods

Study subjects

Patients with CRC (n = 78) were recruited into this study from University of Tsukuba Hospital and Tsukuba Medical Center Hospital (Ibaraki, Japan) between April 2015 and November 2017. Prior to surgery, 20 mL of peripheral blood was collected. The inclusion criterion was a hemoglobin concentration > 100 g/L. Exclusion criteria were viral infection with the human immunodeficiency virus, hepatitis B, or hepatitis C.

Patients were classified by disease stage according to the TNM classification system of malignant tumors published by the International Union Against Cancer. Patient data were registered in an anonymization system at Tsukuba Clinical Research & Development Organization (T-CReDO). Healthy donors (n = 24) were also recruited as a control group from employees of Astellas Pharma, Inc. (Tokyo, Japan) between December 2015 and October 2017. This study was approved by the institutional review board at University of Tsukuba Hospital (No. H26-157), Tsukuba Medical Hospital (No. 2015-036, 2016-044) and Astellas Pharma, Inc. (No. 140032, 150042, 000182), respectively. This study was conducted in accordance with the Declaration of Helsinki.

Written informed consent was obtained from all patients and healthy donors prior to blood drawing.

PBMC isolation

PBMCs were isolated from freshly drawn peripheral blood using BD Vacutainer CPT Mononuclear Cell Preparation Tubes (BD Bioscience, San Jose, CA, USA). The blood samples were centrifuged at 25°C for 15 minutes at 1500 rpm. The isolated PBMCs were washed twice with MACS buffer (Miltenyi Biotech, Gradbach, Germany) containing 10% bovine serum albumin. PBMCs were used immediately for flow cytometric analysis and *in vitro* functional assays without cryopreservation.

Flow cytometry

PBMCs were incubated with human Fc blocker (Miltenyi Biotech) and stained for 20 min at 4°C with the following antibodies: Lin (CD3/CD16/CD19/CD20/CD56)-FITC, CD14-PerCP-Cy5.5, CD11b-APC-Cy7, (BD Bioscience), and HLA-DR-PE (Beckman Coulter, Brea, CA, USA). The PBMCs then were washed twice with MACS buffer and then

analyzed with a FACSVerse flow cytometer with FACSuite software (BD Bioscience). The subsequent data analysis was carried out using FlowJo software (Tree Star, Ashland OR, USA). The gating strategy for mMDSCs is shown in Fig. 2-1.

Plasma protein measurement

Plasma collected during PBMC isolation was frozen in small aliquots at −80°C and subjected to measurement of 27 proteins (IL-1ra; IL-1β; IL-2; IL-4; IL-5; IL-6; IL-7; IL-8; IL-9; IL-10; IL-12p70; IL-13; IL-15; IL-17A; C-C motif chemokine ligand 11 [CCL11; Eotaxin]; fibroblast growth factor 2 [FGF-2]; colony stimulating factor 3 [CSF3; G-CSF]; colony stimulating factor 2 [CSF2; GM-CSF]; interferon gamma [IFN-γ]; tumor necrosis factor alpha [TNF-α]; C-X-C motif chemokine ligand 10 [CXCL10; IP-10]; C-C motif chemokine ligand 2 [CCL2; MCP-1]; C-C motif chemokine ligand 3 [CCL3; MIP-1α]; C-C motif chemokine ligand 4 [CCL4; MIP-1β]; platelet-derived growth factor-BB [PDGF-BB]; regulated on activation, normal T cell expressed and secreted [RANTES]; and vascular endothelial growth factor [VEGF]). These were measured with Bio-Plex Pro Human Cytokine 27-plex (BIO RAD, Hercules, CA, USA). Arginase and iNOS were also

quantified with ELISA (Hycult Biotech, Uden, Netherlands and Cloud-Clone Corp, Houston, TX, USA, respectively).

mMDSC, CD14$^-$ cell, and T cell isolation for *in vitro* mMDSC functional assay

mMDSCs were isolated by a combination of magnetic sorting and flow cytometry. The isolated PBMCs were then mixed with CD14 selection MicroBeads (Miltenyi Biotech, Monocyte Isolation Kit II) and incubated at 4°C for 15 min. The cell suspension was applied onto an LS magnetic column (Miltenyi Biotech). The column was washed with MACS buffer and unlabeled cells that passed through were collected as CD14$^+$ cells. HLA-DR$^{-/low}$CD14$^+$ cells were identified and isolated as mMDSCs using a BD FACSAria III cell sorter (BD Biosciences). The purity of the sorted populations was > 90% in all experiments. CD14$^-$ cells were isolated from PBMCs using CD14 selection Micro beads in parallel with CD14$^+$ cell isolation as above. T cells were isolated from PBMCs using human pan-T cell isolation beads (Miltenyi Biotech, Pan T Cell Isolation Kit) following the manufacturer's protocol; unlabeled cells that passed through were collected as T cells.

***In vitro* mMDSC functional assay**

Autologous mMDSC subsets were added at different ratios to $CD14^-$ cells (5×10^4 cells/well) in 96-well flat bottom plates (Iwaki, Tokyo, Japan) in RPMI 1640 media containing 10% fetal calf serum. Cells were incubated with anti-CD2/anti-CD3/anti-CD28 antibody conjugated beads (Miltenyi Biotech) at a 1:1 $CD14^-$ to bead ratio. Plates were incubated at 37°C in a humidified 5% CO_2 incubator for 5 d. After culture, supernatants were collected and IFN-γ concentration was measured using a human IFN-γ AlphaLISA Detection Kit (Perkin Elmer, Waltham, MA, USA).

For further study, autologous mMDSC subsets (5×10^4 cells/well) were added in a mMDSC:T cell ratio of 1:1 in 96-well flat bottom plates (Iwaki, Tokyo, Japan) in RPMI 1640 media containing 10% fetal calf serum. Cells were incubated with anti-CD2/anti-CD3/anti-CD28 antibody conjugated beads (Miltenyi Biotech) at a 1:1 T-cell to bead ratio. Plates were incubated at 37°C in a humidified 5% CO_2 incubator for 5 d. Supernatants then were collected and IFN-γ concentration was measured using a human IFN-γ AlphaLISA Detection Kit (Perkin Elmer, Waltham, MA, USA).

Statistical analysis

When I analyzed plasma protein concentration, I excluded the measurements from the study whose value = 0 or NA for > 10 subjects, or whose 75th percentile of value was < 10 subjects. The proportion of mMDSCs in PBMCs and concentration of various plasma proteins were log-transformed for analysis. Plasma concentrations of all protein samples below the limit of quantification were assigned to 0.1 to allow log transformation. Statistical comparisons between healthy donors and CRC patients were performed using the 2-sided Welch's *t*-test for continuous variables. Statistical comparisons between mMDSC proportion and categorical variables, such as stage or the site of primary lesions in CRC patients, were conducted using a one-way analysis of variance (ANOVA). A $p < 0.05$ was considered statistically significant. A prediction model against mMDSC proportion in PBMCs was developed applying a multivariate linear regression model. The variables for the regression model were selected using forward and backward stepwise feature selection method from plasma protein measurements and demographic factors (i.e., sex, and age). All statistical analyses were performed using the free statistical software R [47].

Results

mMDSC levels in CRC patients and healthy donors

Table 2-1 shows the characteristics of CRC patients and healthy donors. First, I analyzed the proportion of mMDSCs in the PBMCs. The gating strategy and the representative dot plots for mMDSCs are shown in Fig. 2-1. The percentages of mMDSCs in the PBMCs of the 102 samples from the 78 patients with CRC and the 24 healthy donors were analyzed. The proportion of mMDSCs in the CRC patients was significantly higher than that in the healthy donors ($p < 0.001$; Fig. 2-2).

I assessed for any correlation between mMDSC proportion with TNM tumor stage in CRC patients. CRC patients were divided into four groups based on TNM tumor stage (stage I, II, III and IV [N = 3, 21, 33 and 21, respectively]) for comparison of mMDSC proportion among the groups. Levels of mMDSCs showed no significant differences among tumor stages (Fig. 2-3A). There was no correlation between mMDSC proportion and the site of the primary lesions in CRC patients (Fig. 2-3B). mMDSC proportion was not gender-related (Fig. 2-3C) or age-related (Fig. 2-3D).

Comparison of *in vitro* suppressive function of mMDSCs from CRC patients with those from healthy donors

To confirm peripheral blood mMDSCs from CRC patients and healthy donors suppressed T cell activation, I isolated mMDSCs, $CD14^-$ cells, and pan-T cells from PBMCs and co-cultured them under stimulation with anti-CD2/anti-CD3/anti-CD28 antibody conjugated beads for 5 d. I then assessed the suppressive function of mMDSCs *in vitro*. In mMDSC titration assays (CRC patients, n = 3; healthy donors, n = 3), when autologous mMDSCs were added in an mMDSC:$CD14^-$ cell ratio of 0.25:1, 0.5:1 and 1:1, IFN-γ production of $CD14^-$ cells was inhibited at ratios of 1:1 and 0.5:1. Loss of IFN-γ suppressive activity was observed as mMDSCs were titrated down in both CRC patients and healthy donors (Fig. 2-4A). For further assay (CRC patients: n = 9, healthy donors: n = 5), when autologous mMDSCs were co-cultured with pan-T cells at a ratio of 1:1 (mMDSCs:pan-T cells), IFN-γ production of pan-T-cells was decreased in 4 out of 5 healthy donors and 8 out of 9 CRC patients, confirming mMDSCs' suppressive function irrespective of disease state (Fig. 2-4B and Table 2-2).

Comparison of plasma protein levels between CRC patients and healthy donors

Of the target 29 plasma proteins to be measured, 15, including arginase and iNOS, were detected in CRC patients and healthy donors. The remaining 14 proteins (IL-1b, IL-2, IL-4, IL-5, IL-6, IL-7, IL-10, IL-12p70, IL-13, IL-15, IL-17, MIP-1a, IFN-γ and G-CSF) were excluded from analysis because their value = 0 or NA for > 10 subjects, or whose 75th percentile of value was < 10 subjects. The plasma concentrations of the 15 remaining proteins were compared between CRC patients and healthy donors. Significant differences were observed in the mean plasma levels between the CRC patients and healthy donors for 13 plasma proteins ($p < 0.05$, Table 2-3).

Correlation analysis of mMDSC proportion in CRC patients

First, I conducted univariate correlation analysis to see if there were plasma proteins that were associated with mMDSC proportions in CRC patients, but I did not find any correlation between them (Table 2-4).

Next, I used a multivariate linear regression model, combining forward and backward feature selection based on the AIC (Akaike Information Criterion) to assess

correlations between mMDSC ratios and age, sex, and 15 plasma proteins in CRC patients. The final multivariate linear regression model included iNOS (p = 0.013) and PDGF-BB (p = 0.035) as predictive factors

$$[\log 10\left(\frac{\text{mMDSCs}}{\text{PBMCs}}\right) = 0.2929 - 0.2389 * log10(PDGF - \text{BB}) + 0.3582 * \log 10(\text{iNOS})] \quad (1)$$

(Pearson correlation p < 0.005 and r = 0.32) (Fig. 2-5A).

Of the plasma proteins selected as predictive factors in the multivariate linear regression model, plasma iNOS and PDGF-BB levels in CRC patients were significantly higher than those in healthy donors, although neither protein was associated with mMDSC proportions in CRC patients in univariate analysis (Fig. 2-5B, C and Table 2-4).

Discussion

In agreement with previous reports, my current work has indicated that the proportion of mMDSCs in CRC patients was significantly higher than that in healthy donors. I did not observe significant differences in the proportion of mMDSCs in different tumor stages in CRC patients. Bin Zhang and colleagues previously indicated that mMDSCs in peripheral blood were associated with clinical stage and tumor metastasis in CRC patients. In their study, a significant difference was observed only between patients with advanced tumors and healthy donors while patients with stage I/II cancer had no significant increase in the proportion of circulating mMDSCs [19]. The explanation for the difference in results between my studies and theirs may be due to different sample processing methods or the different markers used in defining mMDSCs. They used whole blood to analyze the percentage of mMDSCs and defined mMDSCs as $Lin^{-/low}HLA\text{-}DR^{-}CD11b^{+}CD33^{+}$ cells. I used PBMCs and defined mMDSCs as $Lin^{-/low}$ $HLA\text{-}DR^{-/low}CD11b^{+}CD14^{+}$ cells. I stained mMDSCs using the method of Kitano and colleagues, who showed that peripheral mMDSC proportion correlated with overall survival in melanoma patients treated with ipilimumab [48]. My study indicates that tumorigenesis significantly affects mMDSC

proportion regardless of clinical stage.

Because validated specific markers for human mMDSCs are still unknown, identification and characterization of mMDSCs requires confirmation of their functional activity [49]. The immunosuppressive properties of mMDSCs are known [50,51], thus measuring T cell inhibition is commonly done. I directly isolated mMDSCs from PBMCs of CRC patients and healthy donors by a two-step method using magnetic bead enrichment followed by flow cytometry. I first isolated $CD14^+$ cells by magnetic sorting and then HLA-$DR^{-/low}$ cells by flow cytometry and used these isolated cells as mMDSCs for *in vitro* co-culture assay with autologous $CD14^-$ cells or T cells isolated separately using magnetic sorting. mMDSC-mediated suppressive activity against IFN-γ production of $CD14^-$ cells increased with increasing percentage of mMDSCs in CRC patients. T cell INF-γ production was reduced by mMDSCs at a 1:1 ratio in 8 out of 9 CRC patients. Interestingly, I found that mMDSCs also suppressed IFN-γ production in healthy donors. These data suggest that the immunosuppressive activity of mMDSCs on a per-cell basis in healthy donors might be comparable to CRC patients' cells, with an increased proportion of mMDSCs in CRC patients would potentiate immune suppression.

In my study, I used fresh PBMCs for analysis because previous studies had emphasized the importance of using fresh blood when monitoring mMDSC proportions in the circulation [18,20,52–54]. For example, Grützner and colleagues showed that freezing PBMCs significantly decreased the yield of mMDSCs [20]. Unfortunately, in clinical practice at present, monitoring mMDSC numbers from fresh PBMCs by flow cytometry with multiple-marker staining on the same day as the blood draw is impractical. Thus, it would be advantageous to develop a simple method to determine mMDSC proportion without using fresh PBMCs. I hypothesized that using plasma from frozen samples might work. I thus assessed whether plasma protein concentrations and demographic factors such as age and sex, would be biomarkers of mMDSC proportion. iNOS and PDGF-BB were predictive of mMDSC proportion. This was consistent with the fact that mMDSCs induce increased levels of NO via iNOS, leading to cell cycle arrest in T cells via depletion of the amino acid l-arginine from the TME [39,55]. It is reported that angiogenic factors such as PDGF-BB have been likely involved in MDSC populations [56]. One of the potential mechanisms is direct expansion from progenitor cells by stimulation of the VEGF receptor [56,57]. Therefore, iNOS and PDGF-BB levels

are potential indicators of mMDSC proportion.

Several groups have reported that mMDSCs were an important prognostic marker for cancer immunotherapy by CPIs such as ipilimumab and nivolumab. In metastatic melanoma patients, mMDSC proportion was utilized to predict clinical response or resistance to ipilimumab treatment [14]. Compared with non-responders, clinical responders to ipilimumab had a significantly lower proportion of mMDSCs in the peripheral blood. This finding suggests the use of peripheral mMDSC proportion as a response marker, because a low MDSC proportion identified patients who benefitted from ipilimumab therapy [14,48]. Other studies also reported that a lower proportion of peripheral mMDSCs at baseline can be used as a predictive marker for ipilimumab therapy for malignant melanoma [58–60]. In castration-resistant prostate cancer patients treated with prostate cancer vaccines and ipilimumab, a low mMDSC proportion in the peripheral blood was reported to be associated with clinical benefit with longer median survival [61]. Weber and colleagues indicated that a higher number of mMDSCs before treatment was associated with a poorer outcome with nivolumab in melanoma [15]. Although there is insufficient information regarding the relationship between peripheral

mMDSC proportion and clinical outcome of CPIs in CRC patients, high levels of peripheral mMDSCs have been reported in this cancer [19,62–64]. Prospective clinical trials assessing mMDSC proportions as potential biomarkers of response to immune checkpoint inhibitors in CRC patients are therefore warranted and further studies involving more CRC patients and other tumor types could validate my observations.

In conclusion, I found that iNOS and PDGF-BB are significant surrogate markers for peripheral mMDSC proportions in CRC patients. My predictive model might contribute to patient stratification in cancer immunotherapy and should guide further research on other populations with different types of malignancies.

Table 2-1. Characteristics of study population

Details of subjects	CRC patients	Healthy donors
Subjects (n)	78	24
CRC stage, (n)		
I	3	-
II	21	-
III	33	-
IV	21	-
Sex, (n)		
Female	24	11
Male	54	13
Age (years), median (range)	66 (42–86)	47.2 (40–55)

(doi: https://doi.org/10.1371/journal.pone.0243643.t001)

Table 2-2 Statistical analysis for suppressive function of mMDSCs

	# of subjects to be tested	# of subjects showing IFN-γ reduction by mMDSCs	Mean of the differences between T cells alone and T cells + mMDSCs	p-value (two-sided paired Welch's *t*-test)	p-value (one-sided binominal test)
Healthy donors	5	4	−73.3	0.362	0.188
CRC patients	9	8	−192.0	0.099	0.020*
Total	14	12	−149.6	0.054	0.006*

* Significant at $p < 0.05$ (doi: https://doi.org/10.1371/journal.pone.0243643.t002)

Table 2-3 Concentration of plasma proteins; comparisons between healthy donors and CRC patients

Plasma proteins	Plasma concentration (log10: [pg/mL]) Mean (SD)		p value (two-sided Welch's *t*-test)
	Healthy donors	CRC patients	
IL-1ra	1.793 (0.281)	1.963 (0.475)	0.034*
IL-8	0.727 (0.739)	1.802 (0.436)	< 0.001*
IL-9	1.275 (0.164)	1.604 (0.363)	< 0.001*
Eotaxin	1.655 (0.293)	1.457 (0.429)	0.013*
FGF basic	1.400 (0.262)	1.581 (0.226)	0.004*
GM-CSF	1.377 (0.811)	1.955 (0.828)	0.004*
IP-10	2.224 (0.174)	2.426 (0.278)	< 0.001*
MCP-1	1.815 (0.677)	1.851 (0.644)	0.818
PDGF-BB	1.877 (0.333)	2.119 (0.342)	0.004*
MIP-1b	1.515 (0.164)	1.754 (0.168)	< 0.001*
RANTES	3.077 (0.220)	3.579 (0.405)	< 0.001*
TNF-α	0.983 (0.306)	1.201 (0.420)	0.008*
VEGF	1.487 (0.765)	1.224 (0.681)	0.140
Arginase	0.942 (0.400)	1.482 (0.413)	< 0.001*
iNOS	2.123 (1.488)	2.819 (0.271)	0.032*

Concentration of plasma proteins (pg/mL) had been transformed by log 10

* Significant at $p < 0.05$ (doi: https://doi.org/10.1371/journal.pone.0243643.t003)

Table 2-4 Univariate analysis in CRC patients: correlation between mMDSC proportion and plasma proteins

Plasma protein	p-value	Pearson's correlation coefficient (r)
IL-1ra	0.326	−0.113
IL-8	0.866	−0.019
IL-9	0.594	−0.061
Eotaxin	0.974	0.004
FGF basic	0.893	0.015
GM-CSF	0.905	−0.014
IP-10	0.915	0.012
MCP-1	0.826	−0.025
PDGF-BB	0.193	−0.149
MIP-1b	0.613	0.058
RANTES	0.612	−0.058
TNF-α	0.449	−0.087
VEGF	0.890	0.016
Arginase	0.794	0.030
iNOS	0.062	0.212

* Significant at $p < 0.05$ (doi: https://doi.org/10.1371/journal.pone.0243643.t004)

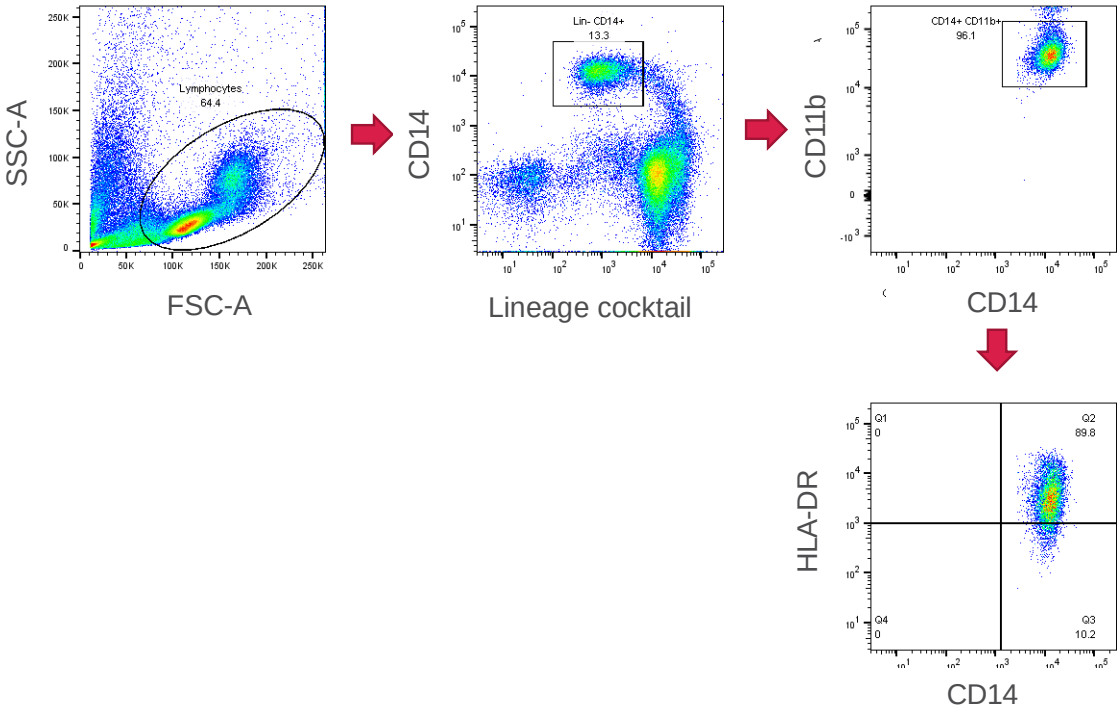

Fig. 2-1 Gating strategy for mMDSC detection

Representative dot plots from flow cytometry to quantitate mMDSCs in PBMCs of healthy donors and CRC patients. (doi: https://doi.org/10.1371/journal.pone.0243643.g001)

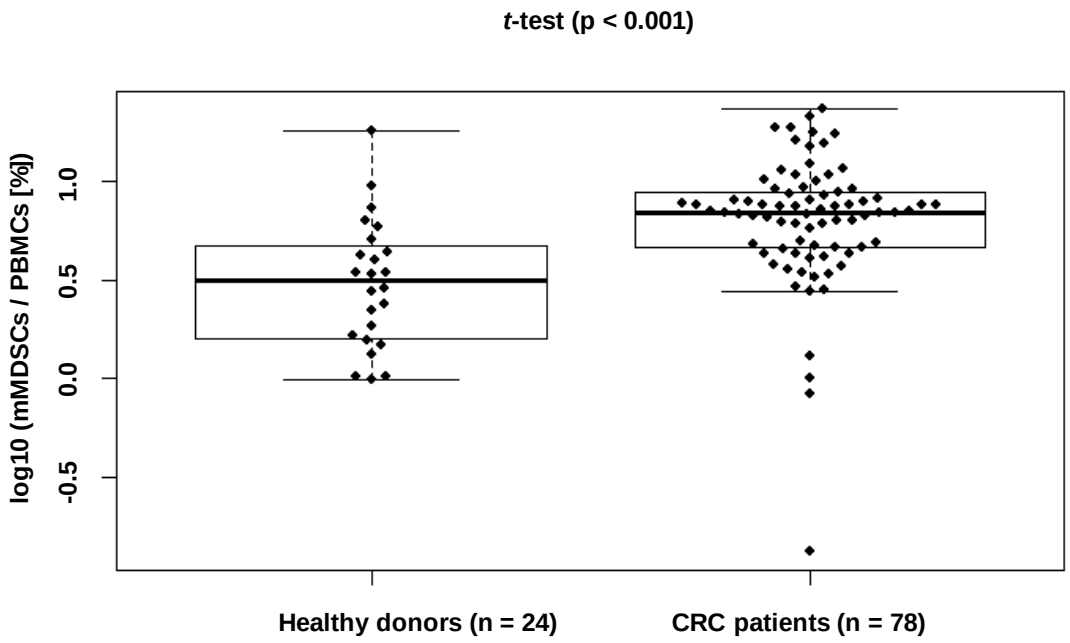

Fig. 2-2 Percentage of circulating mMDSCs in CRC patients and healthy donors.
mMDSC proportion in fresh PBMCs from CRC patients prior to surgery and healthy donors were analyzed. PBMCs from 78 CRC patients and 24 healthy donors were stained for mMDSC markers. mMDSC proportion (% of PBMCs) was transformed by log 10. Data were analyzed by Welch's *t*-test.
(doi: https://doi.org/10.1371/journal.pone.0243643.g002)

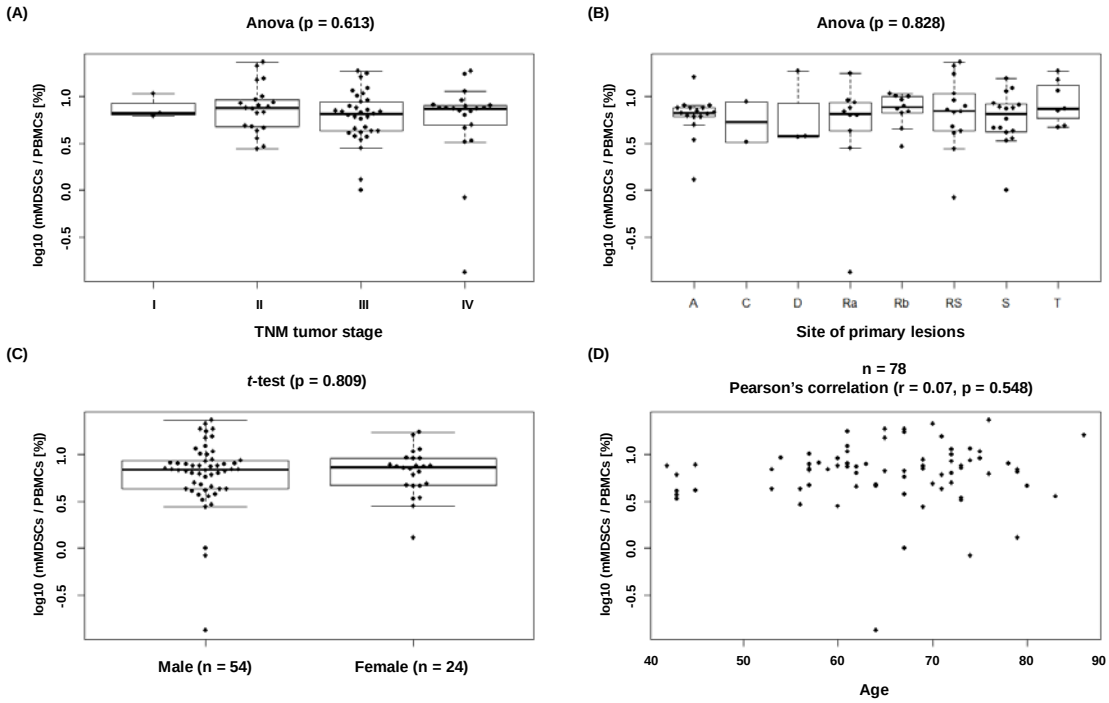

Fig. 2-3 Correlation analyses of mMDSC proportion and stage/demographics in CRC patients

Correlations were assessed between mMDSC proportion and (A) TNM stage, (B) site of the primary lesion, (C) Sex, and (D) Age. mMDSC proportion (% of PBMCs) was transformed by log 10. Data were analyzed by one-way analysis of variance (ANOVA).

(doi: https://doi.org/10.1371/journal.pone.0243643.g003)

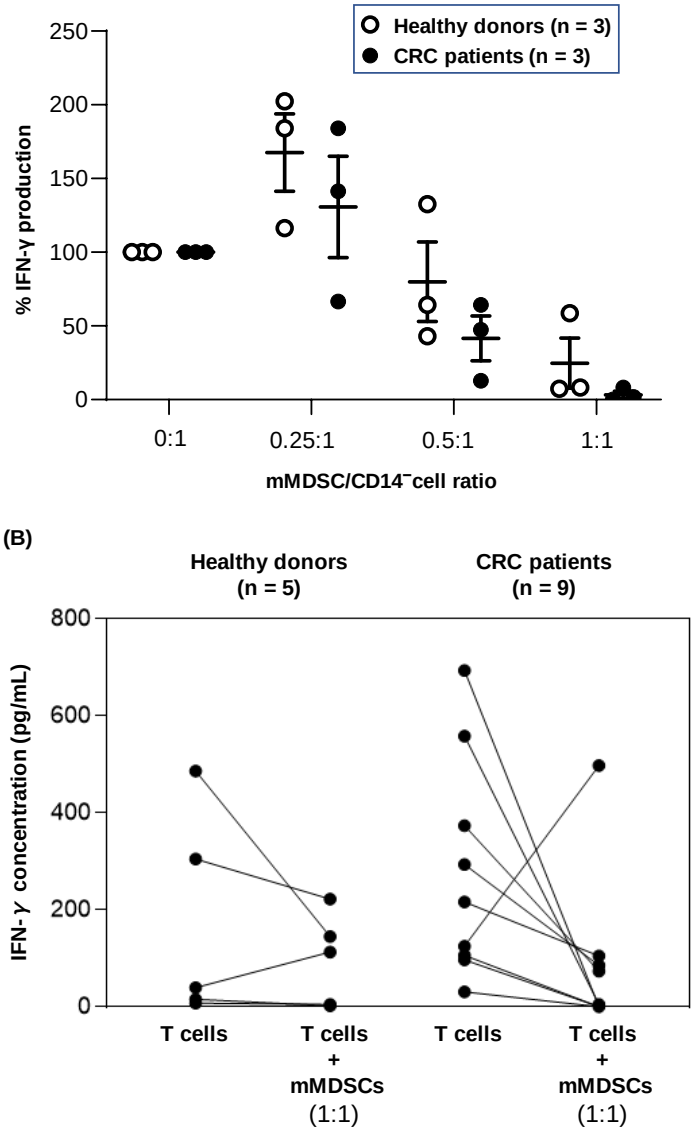

Fig. 2-4 *In vitro* suppressive activity of mMDSCs

(A) $CD14^-$ cells or (B) T cells from healthy donors and CRC patients were stimulated with anti-CD2/anti-CD3/anti-CD28 antibody conjugated beads in the absence or presence of autologous mMDSCs. Culture supernatant was collected at 5 d to measure IFN-γ concentration. (doi: https://doi.org/10.1371/journal.pone.0243643.g004)

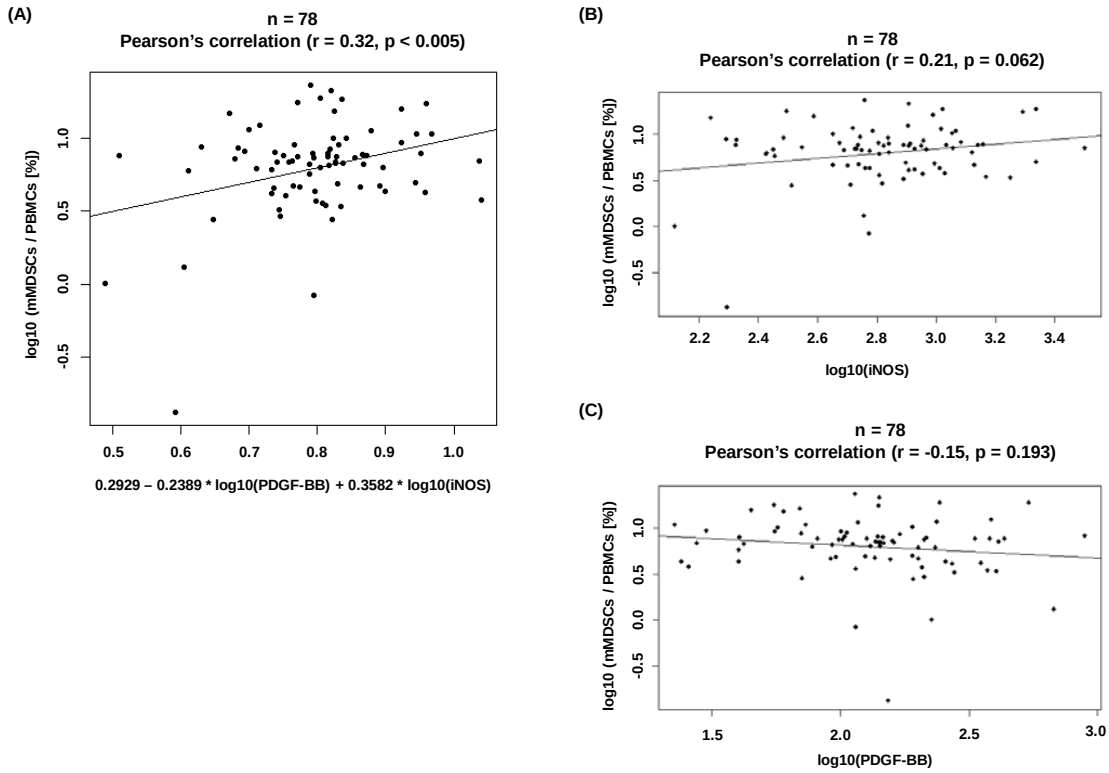

Fig. 2-5 Multivariate analysis for mMDSC proportion in CRC patients

(A) Multivariate linear regression with mMDSC proportion and other factors (plasma proteins, age, gender). Univariate analysis of mMDSC proportion and (B) iNOS and (C) PDGF-BB.

(doi: https://doi.org/10.1371/journal.pone.0243643.g005)

Chapter 3:

Characterization of ASP8374, a Fully-Human, Antagonistic Anti-TIGIT Monoclonal Antibody

Introduction

New therapeutic strategies for the treatment of cancer harness the body's own immune system to mount an anti-tumor response. However, endogenous immune responses are frequently unable to inhibit tumor growth. This deficiency appears to be due to the immunosuppressive nature of the TME. TILs become "exhausted" or suppressed in the context of multiple signals in the TME, resulting in significantly impaired proliferative capacity and effector function [65].s

T cell responses are controlled by various receptor/ligand interactions, and inhibitory or stimulatory signals provided by the TME are excellent drug targets for "reawakening" the immune response to the tumor [66]. Anti-CTLA-4 and anti-PD-(L)1 antibodies have exhibited striking anti-tumor activity in some cancer patients [35,67–69]. These successes have generated increased interest in the identification of additional T cell receptor/ligand

pairs that may regulate T cell function in the TME. Drugs targeting such molecules may provide opportunities for enhanced efficacy in patients who do not adequately respond to currently approved CPI therapy. The costimulatory molecule CD226 and the coinhibitory receptor TIGIT form a costimulatory/coinhibitory pathway analogous to the well-described CD28-CTLA-4 pathway [70,71]. CD226 and TIGIT bind to the same ligands, PVR and PVRL2 [72–74]. Ligand binding to TIGIT induces an inhibitory signal to both the receptor- and ligand-expressing cells. In addition, TIGIT can prevent signaling through CD226, a positive regulator of T cell responses, by competing for binding to PVR [75] (Fig. 1-3). Importantly, upregulated expression of the TIGIT ligands PVR and PVRL2 has been observed in several cancers [76–79], suggesting that this pathway may be utilized by tumors to evade the immune system. Several lines of evidence support an inhibitory role of TIGIT in modulating the immune response. TIGIT is expressed on peripheral memory and regulatory $CD4^+$ and $CD8^+$ T cells and NK cells. It is also upregulated following activation of naïve T cells [75]. TIGIT engagement with PVR or PVRL2 expressed on NK cells inhibits NK cell-mediated cytotoxicity preventing tumor cell death and the subsequent release of tumor-associated antigens [72,74,75]. In addition,

T cells expressing TIGIT interact with dendric cells expressing PVR, inducing tolerogenic dendric cells, impairing T cell proliferation and increasing anti-inflammatory cytokine production [75,80]. TIGIT signal blockade diminishes the immunosuppressive activity of MDSCs and Tregs against $CD8^+$T cells [27–29]. Finally, TIGIT directly inhibits $CD8^+$ T cell activation and proinflammatory $CD4^+$T cell responses in the TME [75,81,82]. ASP8374 is a high affinity, fully human anti-TIGIT IgG4 antibody with S228P hinge stabilization. ASP8374 bound to recombinant human TIGIT with picomolar affinity, increased IL-2 production in TIGIT-expressing Jurkat cells, and increased IFN-γ and TNF-α production in sub-optimally stimulated human PBMCs. Because ASP8374 weakly binds mouse TIGIT, an anti-mouse TIGIT surrogate antibody (mSEC1) was used for mouse tumor studies. mSEC1 demonstrated anti-tumor activity in 2 syngeneic mouse tumor models, either as a single agent or in combination with a PD-1 pathway inhibitor. This non-clinical characterization of ASP8374 suggests it may show efficacy against advanced malignancies in patients.

Materials & Methods

Antibody generation

ASP8374 was isolated from a fully human full length antibody library through the use of a yeast display platform [83]. A surrogate anti-mouse TIGIT antibody (mSEC1) was created using the hamster variable regions from the antibody 10A7 [84], formatted as a mouse IgG2a N297A.

Because ASP8374 bound weakly to mouse TIGIT (data not shown), mSEC1 was used for mouse tumor studies. mSEC1 bound to recombinant mouse TIGIT and bound poorly to human TIGIT, but mSEC1 did cross-block the binding of ASP8374 to human TIGIT, suggesting they may recognize a similar epitope on TIGIT (data not shown).

Binding to recombinant TIGIT

The binding affinities and kinetics of binding of ASP8374 to polyhistidine-tagged TIGIT (TIGIT-His) were measured using Octet QKe (ForteBio). ASP8374 (5 μg/mL) was captured on anti-human IgG Fc (AHC) biosensors (ForteBio) followed by exposure to varying concentrations of human or cynomolgus monkey TIGIT-His (Potenza

Therapeutics). Kinetic parameters were generated with Octet Data Analysis Software (Version 8.2.0.7) using a 1:1 binding model and global fit (Rmax unlinked by sensor).

Binding to cell surface TIGIT

The cell surface binding (K_D) of ASP8374 to human and cynomolgus monkey TIGIT was measured by flow cytometry (LSRFortessa [BD Biosciences]) using Jurkat E6.1 cells overexpressing human or cynomolgus monkey TIGIT. Cells were incubated with ASP8374 or a human IgG4 control antibody labeled with a Zenon antibody labeling kit (Thermo Fisher Scientific). In addition, binding of ASP8374 to cell surface TIGIT on human and cynomolgus monkey PBMCs was conducted with varying concentrations of either ASP8374 or human IgG4 control to calculate K_D values. The secondary staining of human and cynomolgus monkey cells was performed with the following antibodies: CD3 AF700 (Becton Dickenson), CD8 Qdot605 (Biolegend), CD4 APC-Cy7 (eBioscience), and anti-human IgG4 APC (Southern Biotech). For identification of human and cynomolgus $CD8^+$T cells, single cells were gated on expression of CD3 and then on expression of CD8 without expression of CD4. K_D values were calculated using

GraphPad Prism software (Version 7) by plotting the geometric mean fluorescence intensity (MFI) versus logarithmic antibody concentration.

TIGIT ligand competition

Quantitative ligand blocking studies were conducted by using a cell surface TIGIT binding assay. Binding of fluorescently labeled PVR-Fc or PVRL2-Fc to human TIGIT expressing Jurkat cells was measured by flow cytometry. A dilution series of each test antibody was incubated with the TIGIT Jurkat cells in order to measure each antibody's ability to block PVR-Fc or PVRL2-Fc binding. Geometric mean of fluorescence intensity was calculated for each antibody concentration for determination of IC_{50} values in GraphPad Prism.

Jurkat IL-2 production assay

A co-culture stimulation assay was conducted using human TIGIT expressing Jurkat cells and HT-1080 cells that endogenously express PVR and PVRL2 and were engineered to express an anti-CD3 agonist scFv on the cell surface. Cells were treated with ASP8374

or human IgG4 control in the presence of soluble anti-CD28 agonist antibody (R&D Systems) for 24 hours. IL-2 production was measured by ELISA (R&D Systems).

Informed consent

Human PBMCs were obtained from commercial sources with donors' informed consent, in accordance with IRB-approved protocols, and in compliance with all applicable laws and regulations. Subject identification information was masked by providers, and all donor privacy rights were respected. All necessary and appropriate releases were obtained from donors for "Research Use".

PBMC stimulation assay

Human PBMCs obtained from healthy donors by leukapheresis (Biological Specialty Company) were purified and stimulated for 60 hours using a suboptimal concentration of soluble anti-CD3 antibody (0.2 μg/mL) (R&D Systems) in the presence of various concentrations of either the IgG4 control antibody or ASP8374. The concentration of various pro-inflammatory cytokines in the supernatants was measured by ELISA (R&D Systems), AlphaLISA (PerkinElmer), or multiplex/Luminex technology (EMD-

Millipore).

CD4$^+$T cell stimulation assay

Purified CD4$^+$T cells obtained from a healthy donor were stimulated for 60 hours using plate-bound anti-CD3 antibody (1 μg/mL) and soluble anti-CD28 antibody (2 μg/mL) in the presence of different concentrations of either the control IgG4 antibody or ASP8374. The concentration of IFN-γ was measured in supernatants by ELISA (R&D Systems).

CMV-specific immune recall assay

PBMCs from cytomegalovirus (CMV) seropositive human donors (Astarte Biologics) were restimulated with CMV antigens (Astarte Biologics) and treated with either ASP8374 alone or ASP8374 in combination with pembrolizumab. PBMCs were stimulated with CMV lysate (1.0 μg/mL), and supernatants were collected and analyzed for TNF-α production by AlphaLISA after 5 days of culture. In some cases, PBMCs were re-stimulated on day 6 for intracellular cytokine staining analysis.

Jurkat reporter assay

Combination activity of ASP8374 and pembrolizumab was measured *in vitro* using a PD-1/TIGIT Combination Bioassay Kit that contained PD-1/TIGIT expressing Jurkat effector cells and PD-L1/PVR aAPC/CHO-K1 cells (Promega). The effect of combining of ASP8374 and pembrolizumab was evaluated using a luciferase reporter readout. The bioassay was run according to the manufacturer's protocol.

***In vivo* tumor models**

For MC38 studies, female C57BL/6 mice (Charles River Laboratories) were inoculated with $5x10^5$ MC38 cells. The mice (n = 60) were randomized based on tumor volume, and treatment was initiated by intraperitoneal (ip) injection once the tumors reached an average size of 60 – 90 mm^3. For CT26 studies, female BALB/c mice (Charles River Laboratories) were inoculated with $3x10^5$ CT26 cells. The mice (n = 60) were randomized into treatment groups based on body weights, and treatment was initiated by intraperitoneal (ip) injection on the same day as tumor cell inoculation. In both studies, tumors and body weights were measured two times per week. The study endpoint was

defined as day 25 or group mean tumor volume of 2,000 mm^3.

All animal experimental protocols were approved by the Ethics Review Committee for Animal Experimentation of Charles River Laboratories.

Results

ASP8374 binds to TIGIT and enhances T-cell functionality *in vitro*

The binding affinity of ASP8374 for recombinant human and cynomolgus monkey TIGIT was measured using biolayer interferometry. In addition, K_D values for ASP8374 binding to cell surface TIGIT were measured by flow cytometry using engineered cell lines and primary cells (Table 3-1). In both of these assays, ASP8374 potently bound to human and cynomolgus monkey TIGIT.

To confirm the blocking activity of ASP8374 against human TIGIT/ligand interaction, human TIGIT-expressing Jurkat cell binding assay using fluorescently labeled human PVR-Fc or PVRL2-Fc protein was conducted. ASP8374 inhibited the binding of human TIGIT to its ligands (PVR/PVRL2) (Table 3-2).

The antagonistic effect of ASP8374 on TIGIT signaling was investigated in a co-culture assay of human TIGIT-expressing Jurkat cells and anti-CD3 scFv-expressing HT-1080 cells, which endogenously express PVR and PVRL2. In this human co-culture assay, ASP8374 increased the anti-CD3/anti-CD28 antibody-stimulated production of IL-2 with a mean (±SD) EC_{50} of 0.11 (±0.03) nmol/L (Fig. 3-1A).

To test the activity of ASP8374 in human primary cells, PBMCs isolated from healthy donors were stimulated with a sub-optimal concentration of soluble anti-CD3 antibody in the presence of varying concentrations of either the control IgG4 antibody or ASP8374. ASP8374 treatment induced the upregulation of IFN-γ, TNF-α, and lymphotoxin (LT)-α in a titratable manner in a single donor (Fig. 3-1B). To further explore this activity, $CD4^+$T cells isolated from a single donor were sub-optimally stimulated with plate-bound anti-CD3 antibody and soluble anti-CD28 antibody in the presence of various concentrations of either a control IgG4 antibody or ASP8374. In this system, ASP8374 significantly increased IFN-γ production by $CD4^+$ T cells compared to control IgG4 antibody (Fig. 3-1C).

To explore the effects of ASP8374 in an antigen specific assay, PBMCs from two donors who were seropositive for CMV and were known to respond to CMV antigen stimulation were stimulated with CMV lysates for 6 days in the presence or absence of ASP8374. These *in vitro* studies demonstrated that treatment with increasing concentrations of ASP8374 significantly increased PBMC activation as determined by increased TNF-α production (Fig. 3-1D). In addition, ASP8374 treatment increased the

frequency of polyfunctional memory $CD8^+$T cells, identified based on positive intracellular staining of perforin$^+$/granzyme B^+ or IFN-γ^+/TNF-α^+ (Fig. 3-1E).

ASP8374 amplifies anti-PD-1 antibody activity *in vitro*

To determine the functional effect of blocking TIGIT/PVR signaling with ASP8374, PD-1/PD-L1 signaling with pembrolizumab (anti-PD-1 antibody), or both pathways with a combination of both agents, ASP8374 and pembrolizumab were tested alone or in combination in a luciferase reporter gene assay using an engineered functional Jurkat co-culture cell system. ASP8374 in combination with pembrolizumab demonstrated a synergistic effect on luciferase reporter gene expression (Fig. 3-2A and B). The EC_{50} for the combination of ASP8374 and pembrolizumab (fixed 1:1 ratio) was 4.2 nmol/L (Fig. 3A). The EC_{50} for ASP8374 in combination with a fixed concentration of pembrolizumab was 0.1 nmol/L (Fig. 3-2B). In this assay, treatment with pembrolizumab alone resulted in minimal activity, and ASP8374 alone resulted in no activity (Fig. 3-2A and B).

CMV specific $CD8^+$T cells often co-expressed both PD-1 and TIGIT (data not shown). Therefore, to determine whether ASP8374 treatment could amplify the effects of

anti-PD-1 antibody, PBMCs from CMV seropositive donors were stimulated with CMV lysate in the presence of fixed concentration of pembrolizumab and increasing concentrations of either ASP8374 or the IgG4 control antibody. The combination of 40 μg/mL ASP8374 and pembrolizumab led to an approximate 2-fold increase in secreted TNF-α levels compared to control IgG4 treated PBMCs in 2 donors (Fig. 3-2C). These data demonstrate the potential to further amplify the immune response by combining ASP8374 with other CPIs, such as anti-PD-1 antibodies.

TIGIT blockade using an ASP8374 surrogate antibody results in anti-tumor activity

The anti-mouse TIGIT antibody surrogate of ASP8374 (mSEC1) was tested as a monotherapy and in combination with a monoclonal antibody against mouse PD-L1 in the MC38 syngeneic mouse tumor model (anti-PD-(L)1 antibody sensitive model [MDSC low model]). mSEC1 as a monotherapy displayed moderate anti-tumor activity (Fig. 3-3A). However, blockade of PD-1 with an anti-PD-L1 antibody demonstrated exceptionally strong anti-tumor efficacy in the MC38 model. Therefore, the addition of mSEC1 treatment did not further increase anti-tumor activity (Fig. 3-3B). The difference

in the number of mice with complete tumor regression at day 25 between all combination treated groups and the anti-PD-L1 antibody alone treated group was small and not dose-dependent (Table 3-3). Therefore, an additive or synergistic combined effect could not be confirmed in this anti-PD-L1 antibody sensitive mouse model.

To test whether combination therapy could amplify the activity of a PD-1 blocking therapeutic, the activity of these agents was tested in a model where PD-1 blockade is less effective, CT26 (MDSC expansion model). In this model, mSEC1 antibody as monotherapy had no anti-tumor activity (Fig. 3-4A). However, the combination of mSEC1 with anti-PD-1 antibody was more efficacious than either monotherapy on day 25 (Fig. 3-4B). The highest dose of mSEC1 with anti-PD-1 antibody displayed the strongest anti-tumor effect and the largest number of mice with complete tumor regression (Table 3-4).

Discussion

ASP8374 bound to human and cynomolgus monkey TIGIT with high affinity (Table 3-1) and blocked the interaction of TIGIT with PVR and PVRL2 ligands (Table 3-2). The constant region of ASP8374 is a human IgG4 which has low affinity for Fc receptors and is unlikely to result in depletion of TIGIT-positive effector T cells following binding of ASP8374, whereas most clinical stage TIGIT therapeutics are human IgG1, many of which maintain the capacity to induce ADCC [85]. The additional S228P mutation is intended to prevent Fab arm exchange with endogenous IgG4. An antagonistic TIGIT antibody was selected to promote anti-tumor immune responses by reversing the TIGIT/PVR/PVRL2 induced exhaustion of T cells and NK cells [75]. Inhibition of the TIGIT pathway by ASP8374 induced IL-2 production in an engineered human TIGIT Jurkat/anti-CD3 antibody HT-1080 co-culture assay. ASP8374 also increased IFN-γ production in sub-optimally stimulated human PBMCs as well as in $CD4^{+}$T cells isolated from human PBMCs. Furthermore, ASP8374 increased production of IL-2, IFN-γ and TNF-α in a CMV-specific T cell recall response assay. The combination of ASP8374 with an anti-PD-1 antibody further enhanced the TNF-α induction observed in this assay with

either ASP8374 or anti-PD-1 antibody alone.

It is reported that PVR, one of the ligands of TIGIT, is strongly expressed in most human tumor samples of varying types (kidney, stomach, pancreas, skin, brain, lymph node metastases, head and neck squamous cell carcinoma, ovary, bladder, liver, breast, lung) [86]. These data suggest that many tumor types may exploit the TIGIT axis to thwart anti-tumor immune responses in the TME.

To investigate the anti-tumor activity of ASP8374, a surrogate anti-mouse-TIGIT antibody (mSEC1) was designed to mimic ASP8374 with an Fc domain to avoid depletion of immune cells. mSEC1 demonstrated anti-tumor activity in two syngeneic mouse tumor models, either as a single agent or in combination with an anti-PD-1 antibody (Fig. 3-3, 3-4). In the CT26 tumor model (anti-PD-(L)1 antibody insensitive model [MDSC expansion model]) study, anti-PD-1 antibody was modestly active up to day 21, but at the end of the study the mean tumor volume was not different from that of control animals that received a control antibody (Fig. 3-4B). The combination treatment of mSEC1 and an anti-PD-1 antibody enhanced anti-tumor efficacy to CT26 tumors as compared to anti-PD-1 antibody alone, resulting in an increased number of tumor-free mice (Table 3-4).

These data demonstrate that TIGIT blockade can amplify the activity of anti-PD-1 antibody in non-responsive tumor models.

The potential for TIGIT blockade to promote immune responses in the TME is balanced with the potential for invoking systemic immune-related adverse events [87]. TIGIT is a promising target for safe immune checkpoint inhibition, as mice completely lacking TIGIT do not develop autoimmunity [85]. However, blocking TIGIT may impede natural shifting of immune responses toward TH2 [75]. No toxicities were observed in a 5-week repeat-dose study of ASP8374 in cynomolgus monkeys, consistent with other CPI therapy (data not shown).

Taken together, my study results provide evidence that ASP8374 has a therapeutic potential for advanced malignancies with safety.

Table 3-1 Binding affinity of ASP8374 for human and cynomolgus monkey TIGIT

TIGIT Source	**Human** K_D (mol/L)	**Cynomolgus monkey** K_D (mol/L)
Recombinant TIGIT protein	2.4×10^{-10}	6.2×10^{-9}
TIGIT-expressing Jurkat cells	5.1×10^{-10}	4.0×10^{-10}
$CD8^+$T cells	1.3×10^{-9}	2.8×10^{-9}

K_D: dissociation constant

Table 3-2 ASP8374 inhibited interaction of TIGIT with ligands PVR and PVRL2

TIGIT Ligand	**ASP8374 IC_{50} (nmol/L)**
PVR	3.3
PVRL2	1.0

PVR: poliovirus receptor, PVRL2: poliovirus receptor-related 2, IC_{50}: half maximal inhibitory concentration

Table 3-3 Number of tumor-free mice in the MC38 syngeneic mouse model

Treatment	Number of tumor-free mice
Control IgG2b 500 μg	1/10
Anti-PD-L1 125 μg	2/10
mSEC1 62.5 μg + anti-PD-L1 125 μg	6/10
mSEC1 125 μg + anti-PD-L1 125 μg	4/10
mSEC1 250 μg + anti-PD-L1 125 μg	5/10
mSEC1 500 μg + anti-PD-L1 125 μg	3/10

IgG: immunoglobulin G; PD-L1: programmed death-ligand 1; mSEC1: surrogate anti-mouse TIGIT antibody. The number of tumor-free mice (tumor volumes ≤ 4 mm^3) are given for each of the 10 mice per group on day 25.

Table 3-4 Number of tumor-free mice in the CT26 syngeneic mouse model

Treatment	Number of tumor-free mice
Control IgG2b 500 μg	0/10
anti-PD-1 125 μg	1/10
mSEC1 500 μg	0/10
mSEC1 125 μg + anti-PD-1 125 μg	1/10
mSEC1 250 μg + anti-PD-1 125 μg	1/10
mSEC1 500 μg + anti-PD-1 125 μg	4/10

IgG: immunoglobulin G; PD-1: programmed death-1; mSEC1: surrogate anti-mouse TIGIT antibody. The number of tumor-free mice (tumor volumes ≤ 4 mm^3) are given for each of the 10 mice per group on day 43.

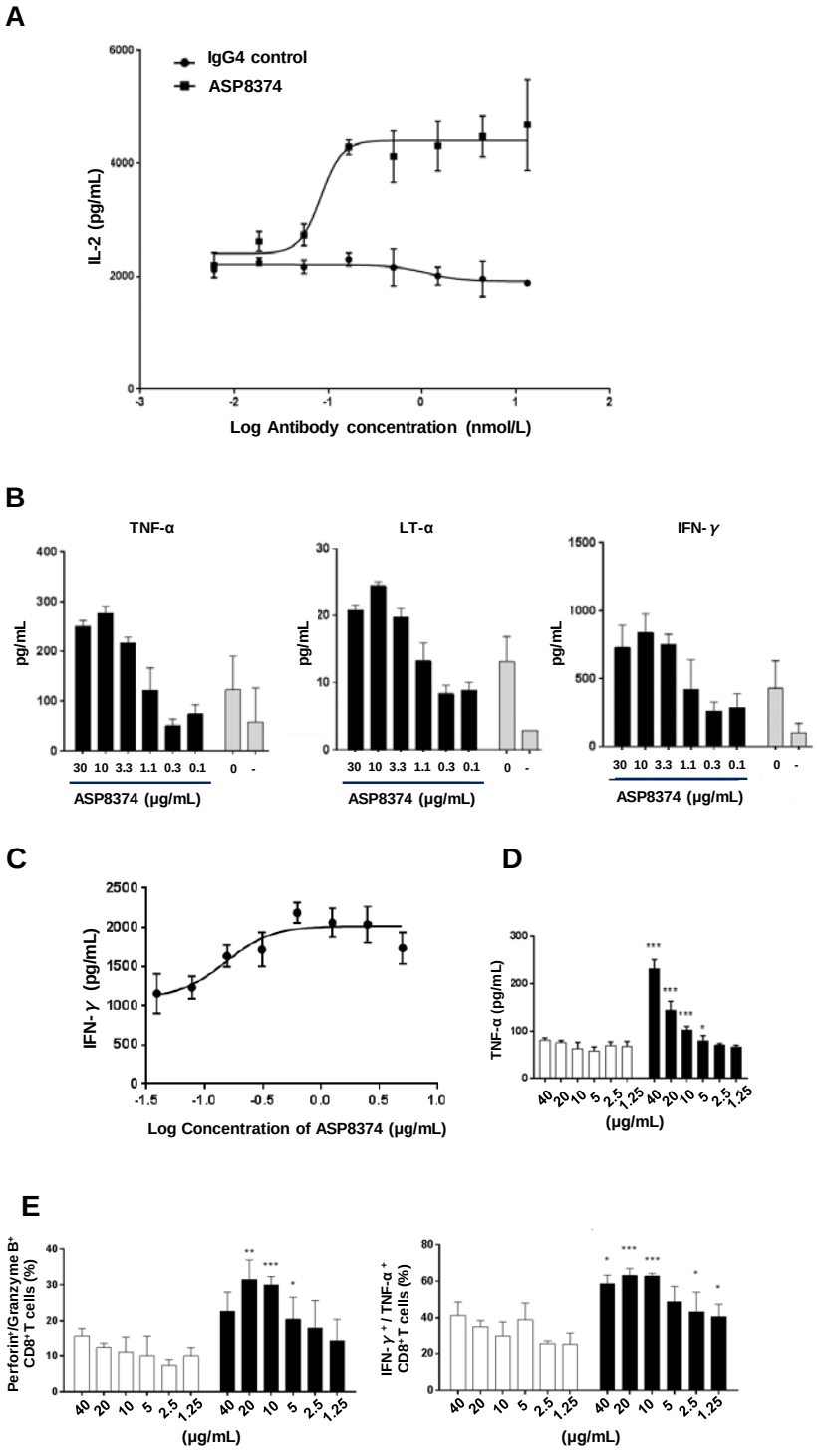

Fig. 3-1. Effect of ASP8374 on immune activation in human cells

(A) ASP8374 antagonizes TIGIT function in an engineered TIGIT Jurkat/anti-CD3 HT-1080 coculture assay. Data are a representative experiment comparing control IgG4 to ASP8374; Half of effective maximal concentration (EC_{50}) of the latter was 0.11 ± 0.03

nM (average ± standard deviation; three replicate experiments). **(B)** PBMCs were stimulated with soluble anti-CD3 antibody for 60 hours in combination with varying concentrations of ASP8374 (black bars), IgG4 (grey bars), or unstimulated (-). Proinflammatory cytokine concentrations were quantified in supernatants. Data labeled '0' indicate the absence of antibody treatment. Data presented are representative of an experiment using cells from a single donor. **(C)** ASP8374 induced the upregulation of IFN-γ production by $CD4^+$T cells. $CD4^+$T cells were sub-optimally stimulated concurrently with various concentrations of a control antibody or ASP8374 for 60 hours, and IFN-γ concentration was measured in supernatants. Data presented are representative of an experiment using cells from a single donor. **(D)** PBMCs from donors previously infected with CMV and shown to be functionally responsive to CMV antigen were stimulated with CMV lysates (1 μg/mL) in the presence of increasing amounts of ASP8374 (black bars) or control antibody (white bars) for 6 days, and TNF-α production in culture supernatant was measured. **(E)** Polyfunctionality of memory $CD8^+$T cells based on perforin$^+$/granzyme B^+ expression (left panel) or IFN-γ^+/TNF-α^+ expression (right panel) was characterized after CMV recall in the presence of increasing amounts of ASP8374 (black bars) or the control antibody (white bars) in cells from an individual donor as in (D) above. *$p < 0.05$; **$p < 0.01$; ***$p < 0.001$, unpaired Student's t-test comparing specific treatment groups to the appropriate IgG4 control.

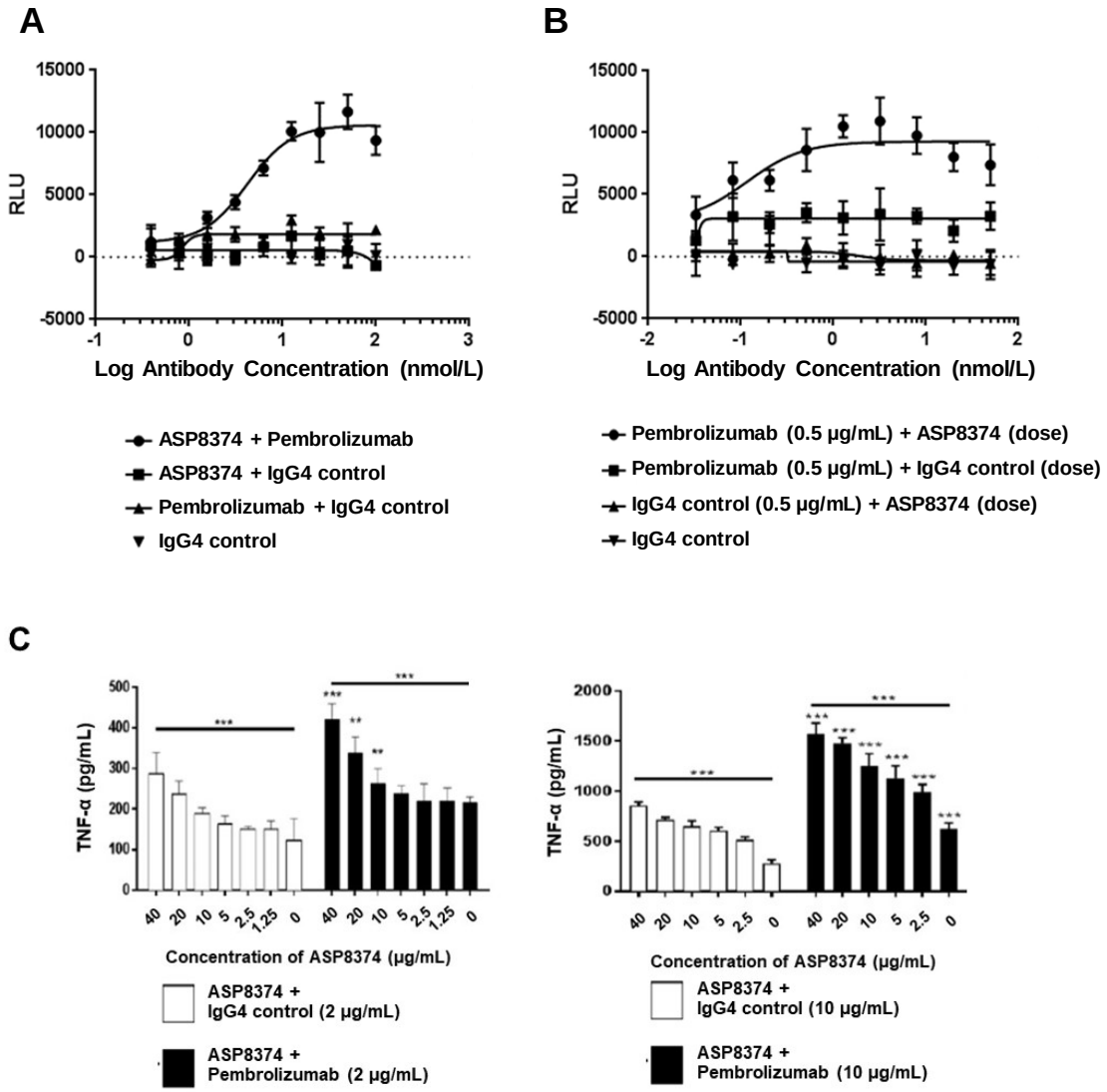

Fig. 3-2 *In vitro* combination effects of ASP8374 with pembrolizumab

(A) The combination activity of ASP8374 and pembrolizumab was investigated in an engineered functional Jurkat co-culture cell assay. Luciferase gene expression in engineered Jurkat/CHO-K1 cells after treatment with increasing amounts of ASP8374 and pembrolizumab at a fixed 1:1 ratio. **(B)** Assay was conducted as in (A), by titration of ASP8374 with a fixed dose of pembrolizumab (0.5 µg/mL). **(C)** Combination activity of ASP8374 and pembrolizumab was investigated in a CMV recall assay. PBMCs from 2 separate donors were treated with increasing amounts of ASP8374 and pembrolizumab at 2 µg/mL (left panel) or 10 µg/mL (right panel) in the presence of the CMV antigen. TNF-α levels in the culture supernatant were used as a measure of primary human T cell activation. *$p < 0.05$, **$p < 0.01$, ***$p < 0.001$; unpaired Student's T test comparing specific treatment groups to the appropriate IgG4 or pembrolizumab control.

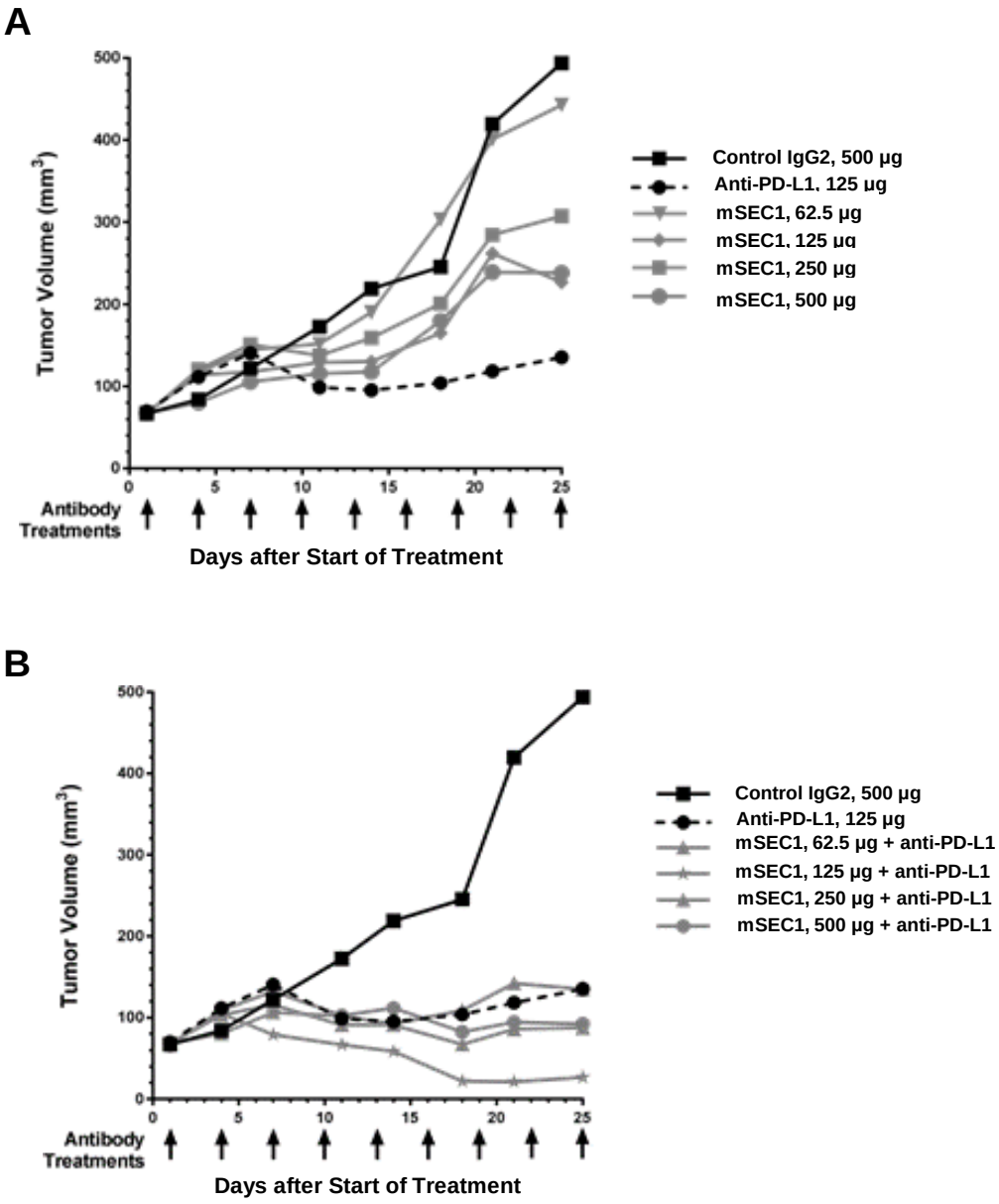

Fig. 3-3 *In vivo* mouse efficacy of anti-TIGIT surrogate antibody in the presence or absence of anti-PD-L1 antibodies in the MC38 colon cancer model

MC38 mouse tumor cells were injected into female C57BL/6 mice (n = 60), randomized into treatment groups and treatment was initiated (Day 1) when average tumor volumes reached 60 mm^3 to 90 mm^3. The average tumor volume of 10 mice/group is shown for each treatment group (A: monoefficacy; B: combination). All antibodies were administered intraperitoneally. Black arrows indicate treatment days.

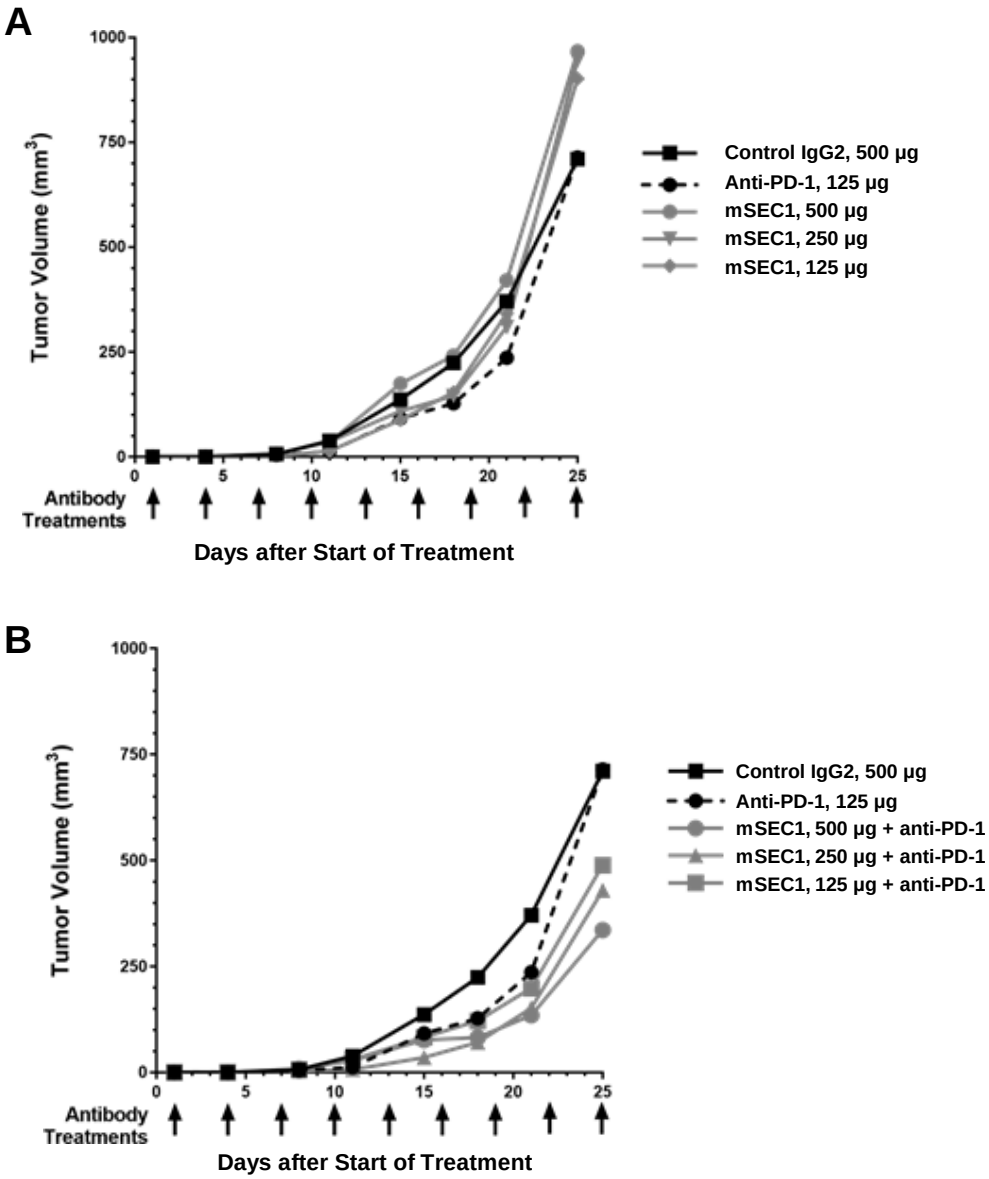

Fig. 3-4 *In vivo* mouse efficacy of anti-TIGIT surrogate antibody in the presence or absence of anti-PD-1 antibodies in the CT26 colon cancer model

CT26 mouse tumor cells were injected into female BALB/c mice (n = 60) on Day 1. Mice were randomized based on body weight and treatments were administered intraperitoneally on the same day. The average tumor volume from 10 mice per group is shown for each treatment group (A: monoefficacy; B: combination). The black arrows indicate treatment days.

General Discussion

Cancer is the second leading cause of death worldwide. Until recently, tumor resection, radiation and chemotherapy have been the three pillars of cancer treatment. However, a fourth pillar, cancer immunotherapy, now exists. This is, in part, due to the fact that it can improve overall survival in some patients with previously refractory cancer. CPIs such as anti-CTLA4 (ipilimumab) and anti-PD-(L)1 (nivolumab, pembrolizumab, atezolizumab, etc.) antibodies, are most promising immunotherapeutic approaches. However, only 20% of cancer patients benefit from current CPI therapy and serious side effects are often observed [11]. Current challenges in CPI therapy are biomarker discovery to enable patient stratification and development of new therapies for CPI-resistant tumors. PD-L1 expression in the tumor site in anti-PD-(L)1 antibody treatment is the only marker now approved for clinical use [13]. Unfortunately, tumor PD-L1 expression is only one step towards predicting the efficacy of anti-PD-(L)1 antibodies in cancer patients. This is because the PD1/PD-L1 interaction is only one of many factors that determine clinical outcome [13]. In biomarker exploration, several groups reported that the peripheral blood mMDSC proportion may be a marker for patient stratification [14,15,18,19,48,58–60].

However, mMDSCs have unstable properties and can only be measured by flow cytometry with complex multicolor staining, a method that is cumbersome to employ in routine clinical laboratory settings.

To identify simpler and more accurate biomarkers, I correlated the percentage of peripheral blood mMDSCs with concentrations of 29 plasma proteins (cytokines, chemokines, and growth factors, etc.) and with age, gender, and tumor stage. I used blood from CRC patients because the number of CRC patients is larger than that of other cancers (including melanoma), blood samples are readily available and high levels of blood mMDSC have been reported in patients with this type of cancer [19,62–64].

My data showed that plasma iNOS and PDGF-BB concentrations correlated with peripheral blood mMDSC proportion (Fig. 2-5A). These results are consistent with those reporting that mMDSCs produce iNOS that reduces l-arginine level in the TME, resulting in the cell cycle arrest of T cells [39,55], and that angiogenic factors, such as PDGF-BB, may be involved in the proliferation of MDSCs [56,57]. Therefore, iNOS and PDGF-BB may be useful predictive factors of peripheral blood mMDSC proportion. In univariate analysis, neither iNOS nor PDGF-BB correlated with the proportion of peripheral blood

mMDSCs. This is probably due to the fact that iNOS is produced by immune cells other than MDSCs [88], and PDGF-BB is produced by endothelial cells, which also have proliferative effects on cells other than MDSCs [89]. This may explain why correlations were observed only through multivariate analysis.

If peripheral blood mMDSC proportion can be predicted from plasma protein concentrations by ELISA, this method would supplant flow cytometry analysis because plasma samples can be kept frozen and ELISA is simple, rapid, and versatile. To put this method to practical use, several steps will be required to improve its accuracy. In addition to the iNOS and PDGF-BB correlations I found, other plasma protein levels also may correlate with peripheral blood mMDSC proportion. I was not able to perform correlation analyses among mMDSC proportion, plasma proteins and CPI efficacy in CRC patients with anti-CTLA4 or anti-PD-(L)1 antibody treatment because these antibodies had not yet been approved in Japan for CRC patients. I hope to do these analyses in the future. Correlation analyses of peripheral mMDSC proportion should be conducted for other cancer types such as melanoma, renal cancer and lung cancer. I hope that my research findings will eventually lead to establishment of a new test method for patient

stratification in current CPI therapy in a wide variety of cancers.

In addition to identifying biomarkers for patient selection in current CPI therapy, novel therapeutic agents that work in patients with tumors that are resistant to current CPIs must be developed. Although the mechanism of resistance is complex and not fully understood, several possibilities have been reported [27]. One of these is that immunosuppressive cells, such as MDSCs and Tregs, are involved in creating an immunosuppressive environment in the tumor site. Several groups demonstrated that intra-tumor MDSC depletion restores the efficacy of anti-PD-1 antibody in mouse models [21,22] and that intra-tumor Treg-depletion or -impairment enhances anti-PD-1 antibody responses [23–25].

TIGIT is a new inhibitory immune checkpoint molecule that is involved in regulation of $CD4^+$, $CD8^+$T cells and NK cells via interaction with its ligands, PVR/PVRL2, which are expressed on cancer cells, MDSCs and dendritic cells [30]. I confirmed that ASP8374 bound to human TIGIT, inhibited the binding of TIGIT to PVR/PVRL2, and improved T cell function in engineered cells and in primary human T cells in *in vitro* (Table 3-1, 3-2, Fig. 3-1). I also confirmed that ASP8374, in combination with an anti-PD-1 antibody

(pembrolizumab), increased T cell activity compared to either agent alone (Fig. 3-2).

Because ASP8374 has no cross-reactivity with mouse TIGIT, an anti-mouse TIGIT surrogate antibody (mSEC1) was generated. To evaluate *in vivo* anti-tumor activity of mSEC1 as a monotherapy and in combination with anti-PD-(L)1 antibodies, two mouse colon tumor models, MC38 (anti-PD-(L)1 antibody sensitive model) and CT26 (anti-PD-(L)1 antibody insensitive model), were tested. mSEC1 as a monotherapy showed anti-tumor activity in the MC38 model (Fig. 3-3). In the CT26 model, mSEC1 alone did not show anti-tumor activity, but in combination of anti-PD-1 antibody, it produced a protective effect than either monotherapy, suggesting that TIGIT blockade can increase the activity of anti-PD-1 antibody in anti-PD-(L)1 insensitive model (Fig. 3-4). The mechanism of combination effect of mSEC1 and anti-PD-1 antibody is unknown. It has been reported that CT26 mice have high levels of MDSC [28], which could explain their resistance to anti-PD-(L)1 antibody therapies. Several groups have reported that TIGIT blockade inhibited the immunosuppressive activity of MDSCs against $CD8^{+}$T cells and NK cells in *in vitro* [29,30,90]. Suppression of MDSC function by TIGIT blockade thus may play a role in the combination effect of mSEC1 and anti-PD-1 antibody.

One of the TIGIT ligands, PVR, is widely expressed in a various type of tumors including kidney, stomach, and pancreatic cancers [86], suggesting that the TIGIT axis may contribute to inhibition of the anti-tumor immune response in patients with many types of tumors.

Although there are concerns about immune-related side effects of blocking inhibitory immune checkpoint functions [91], TIGIT is a promising target because, at least in TIGIT knockout mice [85,87] and cynomolgus monkeys (data not shown), autoimmune effects have been observed. Given the above, ASP8374 has therapeutic potential for advanced malignancies, including anti-PD-(L)1 antibody refractory cancers with safety.

Conclusion

In summary, I demonstrated that measuring the plasma concentrations of iNOS and PDGF-BB may be useful in predicting the proportion of mMDSCs in CRC patients' peripheral blood. My predictive model might contribute to patient stratification in current CPI therapy and should guide further research on populations with other malignancies. The present study also suggested that ASP8374 may exploit the new pathway and improve clinical response with existing immunotherapy such as anti-PD-(L)1 antibodies in the clinic. Clinical trials are currently ongoing, investigating TIGIT blockade for the treatment of patients with several advanced solid tumors. It is my hope that ASP8374, as a monotherapy or in combination with current CPIs, will improve the treatment of patients with CPI-resistant tumors. Eventually, I expect that improvements will be made in my MDSC prediction approach so that proper patient stratification for ASP8374 treatment can be made.

Acknowledgements

I would like to thank Prof. Yasutomi, Prof. Ito, Prof. Yoshiki, Associate Prof. Miyamae and Associate Prof. Hirakawa at the Doctoral Program of Life Science Innovation, School of Integrated and Global Majors, the University of Tsukuba, for their advice, guidance, and coaching on my preparation for this doctoral dissertation.

I would like to thank Dr. Tomura, Senior Vice President, at Candidate Discovery Science Labs., Drug Discovery Research, Astellas Pharma Inc. for giving me an opportunity to participate in the above Doctoral Program and prepare this doctoral dissertation.

I would like to thank Dr. Ito, Dr. Matsuda, Dr. Nishijima, Dr. Kuromitsu, Dr. Koelsch , Dr. Kinugasa, Dr. Sugahara, Dr. Yoshida, Dr. Ohori, Dr. Takeuchi and Dr. Yamaji, at Drug Discovery Research, Astellas Pharma Inc., Dr. Enomoto, Dr. Ohara and Dr. Ohkohchi, at Department of Gastrointestinal and Hepato-Biliary-Pancreatic Surgery, University of Tsukuba Hospital, Dr. Yamamoto, at Ibaraki Western Medical Center, Dr. Dugan, Dr. Salmeron, Dr. Steiner, Dr. Winston, Dr. Brodkin, Dr. Nirschl, Dr. Abbott and Dr. Hicklin, at Potenza Therapeutics for their invaluable advice and guidance.

References

1. Sung H, Ferlay J, Siegel RL, Laversanne M, Soerjomataram I, Jemal A, et al. Global Cancer Statistics 2020: GLOBOCAN Estimates of Incidence and Mortality Worldwide for 36 Cancers in 185 Countries. CA Cancer J Clin. 2021;71(3):209–49.

2. Oiseth SJ, Aziz MS. Cancer immunotherapy: a brief review of the history, possibilities, and challenges ahead. J Cancer Metastasis Treat. 2017;3(10):250.

3. Decker WK, da Silva RF, Sanabria MH, Angelo LS, Guimarães F, Burt BM, et al. Cancer immunotherapy: Historical perspective of a clinical revolution and emerging preclinical animal models. Front Immunol. 2017;8(AUG):829.

4. Gross L. Intradermal Immunization of C3H Mice against a Sarcoma That Originated in an Animal of the Same Line. Cancer Res. 1943;3(5):326–33.

5. Kessler E, Schwartz P, Antebi E. Spontaneous regression of primary malignant melanoma with metastases. Plast Reconstr Surg. 1984;74(3):427–9.

6. Chow MT, Möller A, Smyth MJ. Inflammation and immune surveillance in cancer. Semin Cancer Biol. 2012;22(1):23–32.

7. Halliday GM, Patel A, Hunt MJ, Tefany FJ, Barnetson RSC. Spontaneous regression of human melanoma/nonmelanoma skin cancer: Association with infiltrating CD4+ T cells. World J Surg. 1995;19(3):352–8.

8. Esfahani K, Roudaia L, Buhlaiga N, Del Rincon S V., Papneja N, Miller WH. A review of cancer immunotherapy: From the past, to the present, to the future. Curr Oncol. 2020;27(S2):87–97.

9. Waldman AD, Fritz JM, Lenardo MJ. A guide to cancer immunotherapy: from T cell basic science to clinical practice. Nat Rev Immunol. 2020;20(11):651–68.

10. Buchbinder EI, Desai A. CTLA-4 and PD-1 pathways similarities, differences, and implications of their inhibition. Am J Clin Oncol Cancer Clin Trials. 2016;39(1):98–106.

11. Popovic A, Jaffee EM, Zaidi N. Emerging strategies for combination checkpoint modulators in cancer immunotherapy. J Clin Invest. 2018;128(8):3209–18.

12. Postow MA, Sidlow R, Hellmann MD. Immune-Related Adverse Events Associated with Immune Checkpoint Blockade. Longo DL, editor. N Engl J Med. 2018;378(2):158–68.

13. Singh P, de Souza P, Scott KF, Hall BM, Verma ND, Becker TM, et al. Biomarkers in immune checkpoint inhibition therapy for cancer patients: what is the role of lymphocyte subsets and PD1/PD-L1? Transl Med Commun. 2019;4(1):2.

14. Meyer C, Cagnon L, Costa-Nunes CM, Baumgaertner P, Montandon N, Leyvraz L, et al. Frequencies of circulating MDSC correlate with clinical outcome of melanoma patients treated with ipilimumab. Cancer Immunol Immunother. 2014;63(3):247–57.

15. Weber J, Gibney G, Kudchadkar R, Yu B, Cheng P, Martinez AJ, et al. Phase I/II study of metastatic melanoma patients treated with nivolumab who had progressed after ipilimumab. Cancer Immunol Res. 2016;4(4):345–53.

16. Gabrilovich DI, Nagaraj S. Myeloid-derived suppressor cells as regulators of the immune system. Nat Rev Immunol. 2009;9(3):162–74.

17. Poschke I, Kiessling R. On the armament and appearances of human myeloid-derived suppressor cells. Clin Immunol. 2012;144(3):250–68.

18. Diaz-Montero CM, Salem ML, Nishimura MI, Garrett-Mayer E, Cole DJ,

Montero AJ. Increased circulating myeloid-derived suppressor cells correlate with clinical cancer stage, metastatic tumor burden, and doxorubicin-cyclophosphamide chemotherapy. Cancer Immunol Immunother. 2009;58(1):49–59.

19. Zhang B, Wang Z, Wu L, Zhang M, Li W, Ding J, et al. Circulating and Tumor-Infiltrating Myeloid-Derived Suppressor Cells in Patients with Colorectal Carcinoma. Unutmaz D, editor. PLoS One. 2013;8(2):e57114.

20. Grützner E, Stirner R, Arenz L, Athanasoulia AP, Schrödl K, Berking C, et al. Kinetics of human myeloid-derived suppressor cells after blood draw. J Transl Med. 2016;14(1):2.

21. Kaneda MM, Messer KS, Ralainirina N, Li H, Leem CJ, Gorjestani S, et al. PI3Kγ 3 is a molecular switch that controls immune suppression. Nature. 2016;539(7629):437–42.

22. Steinberg SM, Shabaneh TB, Zhang P, Martyanov V, Li Z, Malik BT, et al. Myeloid cells that impair immunotherapy are restored in melanomas with acquired resistance to BRAF inhibitors. Cancer Res. 2017;77(7):1599–610.

23. Simpson TR, Li F, Montalvo-Ortiz W, Sepulveda MA, Bergerhoff K, Arce F, et al. Fc-dependent depletion of tumor-infiltrating regulatory t cells co-defines the efficacy of anti-CTLA-4 therapy against melanoma. J Exp Med. 2013;210(9):1695–710.

24. Selby MJ, Engelhardt JJ, Quigley M, Henning KA, Chen T, Srinivasan M, et al. Anti-CTLA-4 antibodies of IgG2a isotype enhance antitumor activity through reduction of intratumoral regulatory T cells. Cancer Immunol Res. 2013;1(1):32–42.

25. Bulliard Y, Jolicoeur R, Windman M, Rue SM, Ettenberg S, Knee DA, et al. Activating fc γ receptors contribute to the antitumor activities of immunoregulatory receptor-targeting antibodies. J Exp Med. 2013;210(9):1685–93.

26. Qin S, Xu L, Yi M, Yu S, Wu K, Luo S. Novel immune checkpoint targets: moving beyond PD-1 and CTLA-4. Mol Cancer. 2019;18(1):155.

27. Liu D, Jenkins RW, Sullivan RJ. Mechanisms of Resistance to Immune Checkpoint Blockade. Am J Clin Dermatol. 2019;20(1):41–54.

28. Youn J-I, Nagaraj S, Collazo M, Gabrilovich DI. Subsets of Myeloid-Derived Suppressor Cells in Tumor-Bearing Mice. J Immunol. 2008;181(8):5791–802.

29. Wu L, Mao L, Liu JF, Chen L, Yu GT, Yang LL, et al. Blockade of TIGIT/CD155 signaling reverses t-cell exhaustion and enhances antitumor capability in head and neck squamous cell carcinoma. Cancer Immunol Res. 2019;7(10):1700–13.

30. Sarhan D, Cichocki F, Zhang B, Yingst A, Spellman SR, Cooley S, et al. Adaptive NK cells with low TIGIT expression are inherently resistant to myeloid-derived suppressor cells. Cancer Res. 2016;76(19):5696–706.

31. Simon S, Voillet V, Vignard V, Wu Z, Dabrowski C, Jouand N, et al. PD-1 and TIGIT coexpression identifies a circulating CD8 T cell subset predictive of response to anti-PD-1 therapy. J Immunother Cancer. 2020;8(2):1631.

32. Bray F, Ferlay J, Soerjomataram I, Siegel RL, Torre LA, Jemal A. Global cancer statistics 2018: GLOBOCAN estimates of incidence and mortality worldwide for 36 cancers in 185 countries. CA Cancer J Clin. 2018;68(6):394–424.

33. Mantovani A, Allavena P, Sica A, Balkwill F. Cancer-related inflammation.

Nature. 2008;454(7203).

34. Grivennikov SI, Greten FR, Karin M. Immunity, Inflammation, and Cancer. Cell. 2010;140(6):883–99.

35. Garon EB, Rizvi NA, Hui R, Leighl N, Balmanoukian AS, Eder JP, et al. Pembrolizumab for the Treatment of Non–Small-Cell Lung Cancer. N Engl J Med. 2015;372(21):2018–28.

36. Tosolini M, Kirilovsky A, Mlecnik B, Fredriksen T, Mauger S, Bindea G, et al. Clinical impact of different classes of infiltrating T cytotoxic and helper cells (Th1, Th2, Treg, Th17) in patients with colorectal cancer. Cancer Res. 2011;71(4):1263–71.

37. Schreiber RD, Old LJ, Smyth MJ. Cancer immunoediting: Integrating immunity's roles in cancer suppression and promotion. Science (80-). 2011;331(6024):1565–70.

38. Bronte V, Serafini P, De Santo C, Marigo I, Tosello V, Mazzoni A, et al. IL-4-Induced Arginase 1 Suppresses Alloreactive T Cells in Tumor-Bearing Mice. J Immunol. 2003;170(1):270–8.

39. Corzo CA, Cotter MJ, Cheng P, Cheng F, Kusmartsev S, Sotomayor E, et al. Mechanism Regulating Reactive Oxygen Species in Tumor-Induced Myeloid-Derived Suppressor Cells. J Immunol. 2009;182(9):5693–701.

40. Huang B, Pan PY, Li Q, Sato AI, Levy DE, Bromberg J, et al. Gr-1+CD115+ immature myeloid suppressor cells mediate the development of tumor-induced T regulatory cells and T-cell anergy in tumor-bearing host. Cancer Res. 2006;66(2):1123–31.

41. Kusmartsev S, Nefedova Y, Yoder D, Gabrilovich DI. Antigen-Specific Inhibition of CD8 + T Cell Response by Immature Myeloid Cells in Cancer Is Mediated by Reactive Oxygen Species. J Immunol. 2004;172(2):989–99.

42. Nagaraj S, Schrum AG, Cho H-I, Celis E, Gabrilovich DI. Mechanism of T Cell Tolerance Induced by Myeloid-Derived Suppressor Cells. J Immunol. 2010;184(6):3106–16.

43. Sinha P, Chornoguz O, Clements VK, Artemenko KA, Zubarev RA, Ostrand-Rosenberg S. Myeloid-derived suppressor cells express the death receptor Fas and apoptose in response to T cell-expressed FasL. Blood. 2011;117(20):5381–

90.

44. Gabrilovich DI, Ostrand-Rosenberg S, Bronte V. Coordinated regulation of myeloid cells by tumours. Nat Rev Immunol. 2012;12(4):253–68.

45. Mantovani A. The growing diversity and spectrum of action of myeloid-derived suppressor cells. Eur J Immunol. 2010;40(12):3317–20.

46. Weide B, Martens A, Zelba H, Stutz C, Derhovanessian E, Di Giacomo AM, et al. Myeloid-derived suppressor cells predict survival of patients with advanced melanoma: Comparison with regulatory T cells and NY-ESO-1- or melan-A-specific T cells. Clin Cancer Res. 2014;20(6):1601–9.

47. R: The R Project for Statistical Computing https://www.r-project.org/.

48. Kitano S, Postow MA, Ziegler CGK, Kuk D, Panageas KS, Cortez C, et al. Computational algorithm-driven evaluation of monocytic myeloid-derived suppressor cell frequency for prediction of clinical outcomes. Cancer Immunol Res. 2014;2(8):812–21.

49. Bronte V, Brandau S, Chen S-H, Colombo MP, Frey AB, Greten TF, et al. Recommendations for myeloid-derived suppressor cell nomenclature and

characterization standards. Nat Commun. 2016;7(1):12150.

50. Bruger AM, Dorhoi A, Esendagli G, Barczyk-Kahlert K, van der Bruggen P, Lipoldova M, et al. How to measure the immunosuppressive activity of MDSC: assays, problems and potential solutions. Cancer Immunol Immunother. 2019;68(4):631–44.

51. Yaddanapudi K, Rendon BE, Lamont G, Kim EJ, Rayyan N Al, Richie J, et al. MIF is necessary for late-stage melanoma patient MDSC immune suppression and differentiation. Cancer Immunol Res. 2016;4(2):101–12.

52. Flörcken A, Takvorian A, Singh A, Gerhardt A, Ostendorf BN, Dörken B, et al. Myeloid-derived suppressor cells in human peripheral blood: Optimized quantification in healthy donors and patients with metastatic renal cell carcinoma. Immunol Lett. 2015;168(2):260–7.

53. Mandruzzato S, Solito S, Falisi E, Francescato S, Chiarion-Sileni V, Mocellin S, et al. IL4Rα + Myeloid-Derived Suppressor Cell Expansion in Cancer Patients. J Immunol. 2009;182(10):6562–8.

54. Stanojevic I, Miller K, Kandolf-Sekulovic L, Mijuskovic Z, Zolotarevski L, Jovic

M, et al. A subpopulation that may correspond to granulocytic myeloid-derived suppressor cells reflects the clinical stage and progression of cutaneous melanoma. Int Immunol. 2016;28(2):87–97.

55. Srivastava MK, Sinha P, Clements VK, Rodriguez P, Ostrand-Rosenberg S. Myeloid-derived suppressor cells inhibit T-cell activation by depleting cystine and cysteine. Cancer Res. 2010;70(1):68–77.

56. Markowitz J, Brooks TR, Duggan MC, Paul BK, Pan X, Wei L, et al. Patients with pancreatic adenocarcinoma exhibit elevated levels of myeloid-derived suppressor cells upon progression of disease. Cancer Immunol Immunother. 2015;64(2):149–59.

57. Condamine T, Gabrilovich DI. Molecular mechanisms regulating myeloid-derived suppressor cell differentiation and function. Trends Immunol. 2011;32(1):19–25.

58. Sade-Feldman M, Kanterman J, Klieger Y, Ish-Shalom E, Olga M, Saragovi A, et al. Clinical significance of circulating CD33+ CD11bHLA-DR myeloid cells in patients with stage IV melanoma treated with ipilimumab. Clin Cancer Res.

2016;22(23):5661–72.

59. Gebhardt C, Sevko A, Jiang H, Lichtenberger R, Reith M, Tarnanidis K, et al. Myeloid cells and related chronic inflammatory factors as novel predictive markers in melanoma treatment with ipilimumab. Clin Cancer Res. 2015;21(24):5453–9.

60. Martens A, Wistuba-Hamprecht K, Foppen MG, Yuan J, Postow MA, Wong P, et al. Baseline peripheral blood biomarkers associated with clinical outcome of advanced melanoma patients treated with ipilimumab. Clin Cancer Res. 2016;22(12):2908–18.

61. Santegoets SJ, Stam AG, Lougheed SM, Gall H, Jooss K, Sacks N, et al. Myeloid derived suppressor and dendritic cell subsets are related to clinical outcome in prostate cancer patients treated with prostate GVAX and ipilimumab. J Immunother cancer. 2014;2(1):31.

62. Kanterman J, Sade-Feldman M, Biton M, Ish-Shalom E, Lasry A, Goldshtein A, et al. Adverse immunoregulatory effects of 5FU and CPT11 chemotherapy on myeloid-derived suppressor cells and colorectal cancer outcomes. Cancer Res.

2014;74(21):6022–35.

63. Ma P, Beatty PL, McKolanis J, Brand R, Schoen RE, Finn OJ. Circulating Myeloid Derived Suppressor Cells (MDSC) That Accumulate in Premalignancy Share Phenotypic and Functional Characteristics With MDSC in Cancer. Front Immunol. 2019;10(JUN):1401.

64. Tada K, Kitano S, Shoji H, Nishimura T, Shimada Y, Nagashima K, et al. Pretreatment immune status correlates with progression-free survival in chemotherapy- Treated metastatic colorectal cancer patients. Cancer Immunol Res. 2016;4(7):592–9.

65. Jiang Y, Li Y, Zhu B. T-cell exhaustion in the tumor microenvironment. Cell Death Dis. 2015;6(6):e1792–e1792.

66. Pardoll DM. The blockade of immune checkpoints in cancer immunotherapy. Nat Rev Cancer. 2012;12(4):252–64.

67. Borghaei H, Paz-Ares L, Horn L, Spigel DR, Steins M, Ready NE, et al. Nivolumab versus Docetaxel in Advanced Nonsquamous Non–Small-Cell Lung Cancer. N Engl J Med. 2015;373(17):1627–39.

68. Robert C, Schachter J, Long G V., Arance A, Grob JJ, Mortier L, et al. Pembrolizumab versus Ipilimumab in Advanced Melanoma. N Engl J Med. 2015;372(26):2521–32.

69. Brahmer JR, Drake CG, Wollner I, Powderly JD, Picus J, Sharfman WH, et al. Phase I study of single-agent anti-programmed death-1 (MDX-1106) in refractory solid tumors: Safety, clinical activity, pharmacodynamics, and immunologic correlates. J Clin Oncol. 2010;28(19):3167–75.

70. Lozano E, Dominguez-Villar M, Kuchroo V, Hafler DA. The TIGIT/CD226 Axis Regulates Human T Cell Function. J Immunol. 2012;188(8):3869–75.

71. Levin SD, Taft DW, Brandt CS, Bucher C, Howard ED, Chadwick EM, et al. Vstm3 is a member of the CD28 family and an important modulator of T-cell function. Eur J Immunol. 2011;41(4):902–15.

72. Stanietsky N, Rovis TL, Glasner A, Seidel E, Tsukerman P, Yamin R, et al. Mouse TIGIT inhibits NK-cell cytotoxicity upon interaction with PVR. Eur J Immunol. 2013;43(8):2138–50.

73. Stengel KF, Harden-Bowles K, Yu X, Rouge L, Yin J, Comps-Agrar L, et al.

Structure of TIGIT immunoreceptor bound to poliovirus receptor reveals a cell-cell adhesion and signaling mechanism that requires cis-trans receptor clustering. Proc Natl Acad Sci U S A. 2012;109(14):5399–404.

74. Stanietsky N, Simic H, Arapovic J, Toporik A, Levy O, Novik A, et al. The interaction of TIGIT with PVR and PVRL2 inhibits human NK cell cytotoxicity. Proc Natl Acad Sci U S A. 2009;106(42):17858–63.

75. Manieri NA, Chiang EY, Grogan JL. TIGIT: A Key Inhibitor of the Cancer Immunity Cycle. Trends Immunol. 2017;38(1):20–8.

76. Oshima T, Sato S, Kato J, Ito Y, Watanabe T, Tsuji I, et al. Nectin-2 is a potential target for antibody therapy of breast and ovarian cancers. Mol Cancer. 2013;12(1):60.

77. Bevelacqua V, Bevelacqua Y, Candido S, Skarmoutsou E, Amoroso A, Guarneri C, et al. Nectin like -5 overexpression correlates with the malignant phenotype in cutaneous melanoma. Oncotarget. 2012;3(8):882–92.

78. Casado JG, Pawelec G, Morgado S, Sanchez-Correa B, Delgado E, Gayoso I, et al. Expression of adhesion molecules and ligands for activating and

costimulatory receptors involved in cell-mediated cytotoxicity in a large panel of human melanoma cell lines. Cancer Immunol Immunother. 2009;58(9):1517–26.

79. Sloan KE, Eustace BK, Stewart JK, Zehetmeier C, Torella C, Simeone M, et al. CD155/PVR plays a key role in cell motility during tumor cell invasion and migration. BMC Cancer. 2004;4(1):73.

80. Yu X, Harden K, Gonzalez LC, Francesco M, Chiang E, Irving B, et al. The surface protein TIGIT suppresses T cell activation by promoting the generation of mature immunoregulatory dendritic cells. Nat Immunol. 2009;10(1):48–57.

81. Kurtulus S, Sakuishi K, Ngiow SF, Joller N, Tan DJ, Teng MWL, et al. TIGIT predominantly regulates the immune response via regulatory T cells. J Clin Invest. 2015;125(11):4053–62.

82. Joller N, Lozano E, Burkett PR, Patel B, Xiao S, Zhu C, et al. Treg cells expressing the coinhibitory molecule TIGIT selectively inhibit proinflammatory Th1 and Th17 cell responses. Immunity. 2014;40(4):569–81.

83. Adimab web site https://www.adimab.com/.

84. Novel compositions and methods for the treatment of immune related diseases.

USA; US 2009/0258013 A1, 2009.

85. Chauvin J-M, Zarour HM. TIGIT in cancer immunotherapy. J Immunother Cancer. 2020;8(2):e000957.

86. Gao J, Zheng Q, Xin N, Wang W, Zhao C. CD155, an onco-immunologic molecule in human tumors. Cancer Sci. 2017;108(10):1934–8.

87. Rotte A, Jin JY, Lemaire V. Mechanistic overview of immune checkpoints to support the rational design of their combinations in cancer immunotherapy. Ann Oncol. 2018;29(1):71–83.

88. Cinelli MA, Do HT, Miley GP, Silverman RB. Inducible nitric oxide synthase: Regulation, structure, and inhibition. Med Res Rev. 2020;40(1):158–89.

89. Woo SL-Y, Mau JR, Kang H, Liang R, Almarza AJ, Fisher MB. Functional Tissue Engineering of Ligament and Tendon Injuries. Princ Regen Med. 2019;1179–98.

90. Sarhan D, Brandt L, Felices M, Guldevall K, Lenvik T, Hinderlie P, et al. 161533 TriKE stimulates NK-cell function to overcome myeloid-derived suppressor cells in MDS. Blood Adv. 2018;2(12):1459–69.

91. Nakamura Y. Biomarkers for immune checkpoint inhibitor-mediated tumor response and adverse events. Front Med. 2019;6:1–18.